EPHB6 controls catecholamine biosynthesis by up-regulating tyrosine hydroxylase transcription in adrenal gland chromaffin cells

Received for publication, September 18, 2018, and in revised form, February 25, 2019 Published, Papers in Press, March 1, 2019, DOI 10.1074/jbc.RA118.005767

Wei Shi[‡], **Yujia Wang**[‡§], **Junzheng Peng**[‡], **Shijie Qi**[‡], **Nicolas Vitale**[¶], **Norio Kaneda**[‖], **Tomiyasu Murata**[‖], **Hongyu Luo**[‡1], **and Jiangping Wu**[‡**2]

From the [‡]*Research Centre and* **Nephrology Department, Centre Hospitalier de l'Université de Montréal Montreal, Quebec, H2X 0A9, Canada, the* [§]*Children's Hospital, Zhejiang University School of Medicine, Hangzhou, Zhejiang 310003, China, the* [¶]*Institut des Neurosciences Cellulaires et Intégratives, UPR-3212, CNRS-Université de Strasbourg, 5 rue Blaise Pascal, 67000 Strasbourg, France, and the* [‖]*Department of Analytical Neurobiology, Faculty of Pharmacy, Meijo University, Tempaku, Nagoya 4688503, Japan*

Edited by John M. Denu

EPHB6 is a member of the erythropoietin-producing hepatocellular kinase (EPH) family and a receptor tyrosine kinase with a dead kinase domain. It is involved in blood pressure regulation and adrenal gland catecholamine (CAT) secretion, but several facets of EPHB6-mediated CAT regulation are unclear. In this study, using biochemical, quantitative RT-PCR, immunoblotting, and gene microarray assays, we found that EPHB6 up-regulates CAT biosynthesis in adrenal gland chromaffin cells (AGCCs). We observed that epinephrine content is reduced in the AGCCs from male Ephb6-KO mice, caused by decreased expression of tyrosine hydroxylase, the rate-limiting enzyme in CAT biosynthesis. We demonstrate that the signaling pathway from EPHB6 to tyrosine hydroxylase expression in AGCCs involves Rac family small GTPase 1 (RAC1), MAP kinase kinase 7 (MKK7), c-Jun N-terminal kinase (JNK), proto-oncogene c-Jun, activator protein 1 (AP1), and early growth response 1 (EGR1). On the other hand, signaling via extracellular signal–regulated kinase (ERK1/2), p38 mitogen-activated protein kinase, and ELK1, ETS transcription factor (ELK1) was not affected by EPHB6 deletion. We further report that EPHB6's effect on AGCCs was via reverse signaling through ephrin B1 and that EPHB6 acted in concert with the nongenomic effect of testosterone to control CAT biosynthesis. Our findings elucidate the mechanisms by which EPHB6 modulates CAT biosynthesis and identify potential therapeutic targets for diseases, such as hypertension, caused by dysfunctional CAT biosynthesis.

EPHB6 is a member of erythropoietin-producing hepatocellular kinases (EPHs),[3] the largest family of receptor tyrosine kinases (1, 2). The ligands of EPH are called ephrins (EFNs), which are also membrane proteins. EFNs can trigger EPH signaling by canonical forward signaling, *i.e.* from ligand EFNs to receptor EPHs. However, EFNs can also receive signaling from EPHs and transduce signals into cells, and such noncanonical action (*i.e.* from EPHs to EFNs) is called reverse signaling (2). The interaction between EPHs and EFNs is promiscuous; one EPH can bind to multiple EFNs and one EFN to multiple EPHs. In general, EPHA family members bind to EFNAs, and EPHB family members binds to EFNBs (2).

EPHs/EFNs function in many organs and systems (2). We first reported the critical involvement of EPHs and EFNs in the immune system (3–15). In the past 5 years, we have demonstrated in a series of publications (16–25) that EPHs/EFNs are involved in regulating blood pressure (BP), which was previously unknown. We reported, using gene knockout mouse models, that although EPHB6, EFNB1, EFNB3, and EPHA4 deletion results in BP elevation (16, 17, 20, 25), EPHB4 and EFNB2 deletion lowers it (18, 19). Thus, members of EPHBs/EFNBs are a novel yin and yang system that fine-tunes BP homeostasis. In all such cases, sex hormones act in concert with these EPHs/EFNs to control BP. Some of the findings from the mouse model have been corroborated by human genetic studies, in which we revealed that some variants in the EFNB2, EFNB3, and EPHA4 genes or a related signaling molecule gene are significantly associated with hypertension in a sex-specific way (19, 21, 22, 24, 25).

EPHB6 is highly expressed in the medullae of adrenal glands, which are the major source of catecholamine (CAT) in the circulation. The ambient blood CAT level reflects this hormone's effect on the homeostasis of BP (26, 27). We showed that male

This work was supported by the Fonds de Recherche du Québec–Santé (to J. W. and H. L.) and the J.-Louis Lévesque Foundation (to J. W.). It was also funded in part by grants from the Canadian Institutes of Health Research (MOP272014 to J. W.) and the Natural Sciences and Engineering Research Council of Canada (RGPIN-2017-04790) and the Juvenile Diabetes Research Foundation (17-2013-440) (to J. W.). The authors declare that they have no conflicts of interest with the contents of this article.

The array data were deposited into the GEO with accession number GSE120400.

[1] To whom correspondence may be addressed: CRCHUM, 900 rue St-Denis, R12-426, Montreal, QC H2X 0A9, Canada. Tel.: 514-890-8000, extension 25319; E-mail: hongyu.luo@umontreal.ca.

[2] To whom correspondence may be addressed: CRCHUM, 900 rue St-Denis, R12-428, Montreal, QC H2X 0A9, Canada. Tel.: 514-890-8000, extension 25164; E-mail: jianping.wu@umontreal.ca.

[3] The abbreviations used are: EPH, erythropoietin-producing hepatocellular kinase; EFN, ephrin; BP, blood pressure; CAT, catecholamine; AGCC, adrenal gland chromaffin cell; ACh, acetylcholine; BK, big potassium; TH, tyrosine hydroxylase; RT-qPCR, quantitative RT-PCR; nAChR, nicotinic acetylcholine receptor; mAChR, muscarinic acetylcholine receptor; JNK, c-Jun N-terminal kinase; ERK, extracellular signal–regulated kinase; MAPK, mitogen-activated protein kinase; Ab, antibody; VGCC, voltage-gated calcium channel; SRE, serum-responsive element; FCS, fetal calf serum.

Ephb6 gene KO mice produce reduced amounts of 24-h urinary CAT (16), but such a phenotype disappears after castration (16). We further demonstrated that CAT release in male KO adrenal gland chromaffin cells (AGCCs) is decreased as a consequence of compromised Ca^{2+} influx triggered by acetylcholine (ACh) (23). This decrease was caused by EPHB6 deletion in combination with the nongenomic effect of testosterone, and, hence, after castration or in females, CAT secretion by KO AGCCs is normal (16). We further demonstrated that reduced Ca^{2+} influx in male KO AGCCs is the result of augmented big potassium (BK) channel current, which causes earlier closure of voltage-gated calcium channels, leading to decreased Ca^{2+} influx (23).

In this study, we report that EPHB6 also plays a critical role in regulating CAT biosynthesis. The signaling pathway from EPHB6 to CAT biosynthesis was investigated.

Results

Adrenal glands from male Ephb6 KO mice showed reduced epinephrine content

Our previous study demonstrated that male but not female *Ephb6* KO mice have reduced CAT secretion (16). Secretion and biosynthesis of CAT are distinct but interrelated events. To assess whether the KO adrenal glands were also compromised in CAT biosynthesis, we measured their CAT content using epinephrine as a representative CAT, as our previous study showed that the levels of three major types of CAT (epinephrine, norepinephrine, and dopamine) in the 24-h urine were similarly reduced in male KO mice. As shown in Fig. 1*A*, the epinephrine content in male KO but not female KO adrenal glands was significantly reduced, but castration brought the level of male KO AGCCs to that seen in uncastrated WT counterparts. This pattern is consistent with that of 24-h urine CAT levels in KO mice before and after castration (16). The size of adrenal gland medullae from male, female, and castrated male KO mice was similar to their WT counterparts (Fig. 1*B*), suggesting that the change in epinephrine content in male KO mouse adrenal glands is not due to altered size of the gland medullae.

We then investigated whether the reduced epinephrine content in the male KO adrenal glands was due to the decreased levels of TH, the rate-limiting enzyme in CAT biosynthesis. As shown in Fig. 1*C*, the TH mRNA levels were decreased in the male but not female KO glands compared with their WT counterparts. Such a decrease was abolished after castration.

This pattern of TH expression was also confirmed at the protein level (Fig. 1*D*). Therefore, EPHB6 deletion correlated with reduced TH expression in a male sex hormone–dependent fashion, TH being the rate-limiting enzyme of CAT biosynthesis.

Ephb6 KO decreased expression of the transcription factor Egr1 in adrenal gland medullae

To elucidate the molecular mechanisms underlying the defective TH expression in adrenal gland medullae, we subjected WT and KO medullae to transcriptome microarray analysis. Because TH expression was decreased in male but not female KO medullae, and because such a change disappeared after castration, we sought out genes whose expression pattern fit this pattern, *i.e.* they were altered in male but not female KO medullae, and such alteration in males would disappear after castration. We first compared the gene expression profile of male WT and KO adrenal gland medullae. Twenty genes had more than 2-fold higher expression in WT medullae than in KO medullae, but none had more than 2-fold lower expression with such comparison, as shown in the heatmap in Fig. 2*A*, *left panel*, *left column*. The expression of these 20 genes in female WT *versus* KO medullae and in castrated WT *versus* castrated KO medullae was then compared (Fig. 2*A*, *left panel*, *center* and *right columns*). Only two genes (*LOC666403* and *CFD*) still showed more than 2-fold higher expression in female WT and castrated WT medullae compared with their KO counterparts. The remaining 18 genes resembled the expression pattern for which we were looking and could potentially be involved in regulating TH expression.

We selected the top four hits from the 18 genes for further investigation. The selection criterion was that they had to have more than 3-fold higher expression in male WT medullae compared with KO ones (*i.e. Egr1*, 11.1-fold; *JunB*, 5.8-fold; *Fos*, 3.8-fold; and *Dusp1*, 3.2-fold). The first three are transcription factors, and the last one is a phosphatase. Although *Hspa1a* had a similar high-level change (3.5-fold) because of the ubiquitous presence of this heat shock protein and it being neither a transcription factor nor an enzyme, it was excluded from further study.

Even though we could confirm by RT-qPCR that the mRNA expression of *JUNB*, *FOS*, and *DUSP1* was significantly reduced in male KO medullae, their protein levels showed no change (data not shown). Therefore, no further investigation was carried out on these three genes.

We confirmed by RT-qPCR that *Egr1* mRNA expression was significantly lower in male but not in female KO medullae compared with their WT counterparts (Fig. 2*B*). This decrease was ameliorated after castration. This was verified at the protein level by immunoblotting (Fig. 2*C*), *i.e.* male but not female KO medullae had lower EGR1 protein level, and this was reversed to normal levels after castration.

Reduced EGR1 expression in KO chromaffin cells was correlated with decreased TH expression

EGR1 is a transcription factor. To prove that a reduced EGR1 level was responsible for the decreased TH expression and, hence, reduced CAT biosynthesis, we knocked down EGR1 expression by siRNA in a nonmalignant mouse AGCC cell line (tsAM5NE) (28). The efficiency of *Egr1*/EGR1 knockdown at the mRNA and protein levels was confirmed by RT-qPCR and immunoblotting (Fig. 3*A*). As a consequence of EGR1 knockdown, TH expression at the mRNA and protein level was reduced (Fig. 3*B*), indicating that the EGR1 transcription factor is indeed responsible for enhancing TH mRNA transcription. It is to be noted that tsAM5NE cells, although being normal AGCCs, only produce norepinephrine but not epinephrine (28), and therefore, the former was used as a surrogate representative of CAT in our assay. The norepinephrine content in the tsAM5NE cells was decreased as expected (Fig. 3*C*) after EGR1 knockdown as a consequence

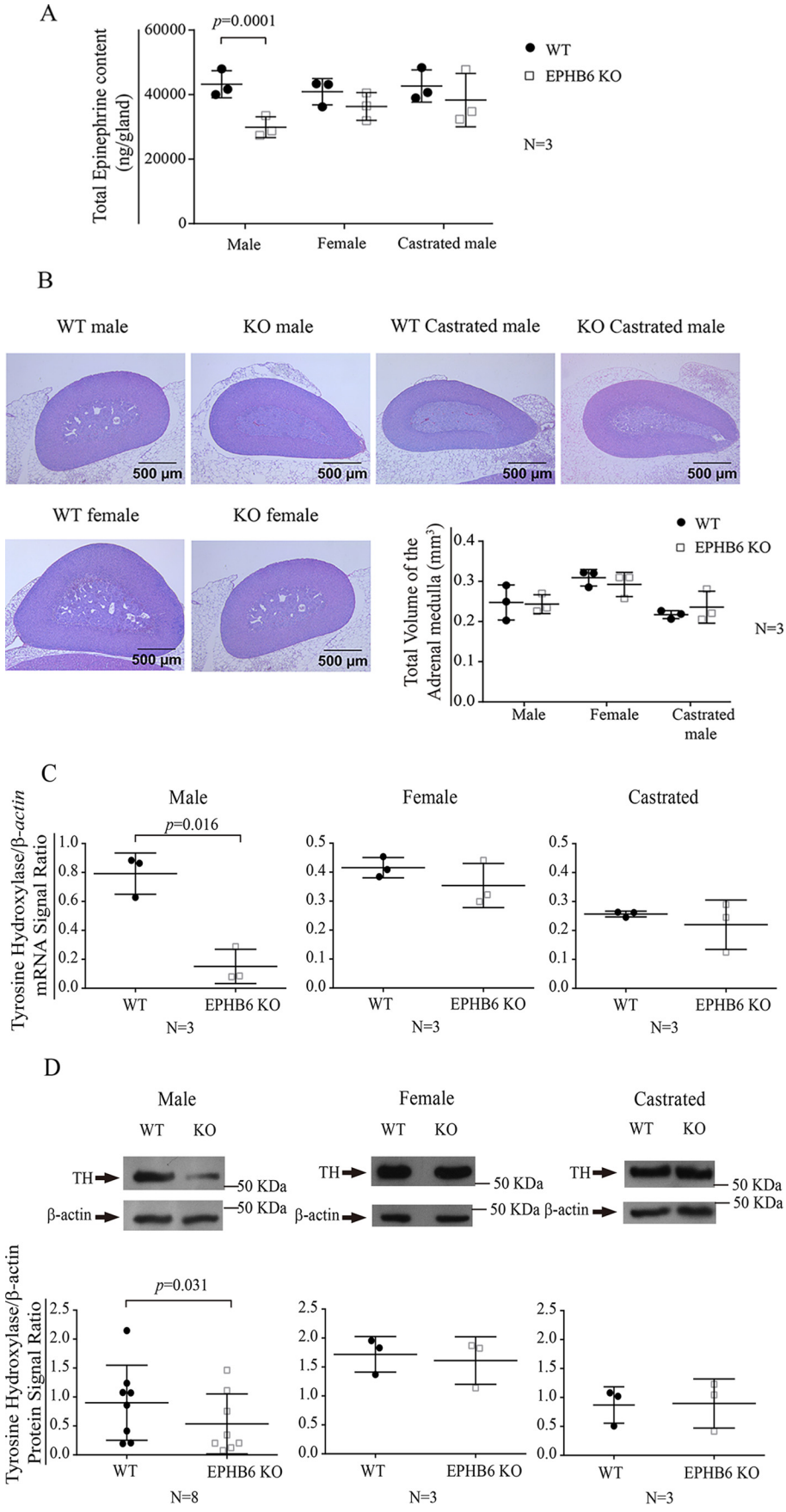
A
p=0.0001
Total Epinephrine content (ng/gland)
60000
40000
20000
0
Male
Female
Castrated male
WT
EPHB6 KO
N=3
B
WT male
KO male
WT Castrated male
KO Castrated male
500 µm
WT female
KO female
Total Volume of the Adrenal medulla (mm³)
0.4
0.3
0.2
0.1
0.0
Male
Female
Castrated male
WT
EPHB6 KO
N=3
C
Male
Female
Castrated
p=0.016
Tyrosine Hydroxylase/β-actin mRNA Signal Ratio
1.0
0.8
0.6
0.4
0.2
0.0
WT
EPHB6 KO
N=3
D
Male
Female
Castrated
WT
KO
TH
β-actin
50 KDa
Tyrosine Hydroxylase/β-actin Protein Signal Ratio
p=0.031
2.5
2.0
1.5
1.0
0.5
0.0
N=8
N=3

of reduced TH level. Thus, these results show that reduced EGR1 expression is correlated with reduced CAT synthesis in AGCCs from *Ephb6* KO mice.

Ephb6 KO leads to reduced AP-1 association with its binding site in the Egr1 gene enhancer

One possible mechanism by which *EPHB6* may control *Egr1* expression is that it acts through transcription factors, which associate with *Egr1* gene enhancers. There is an AP-1 binding site between positions +383 and +393 in the 5′ UTR of the *Egr1* gene. AP-1 promotes gene transcription when bound to enhancers, *i.e.* AP-1 binding sites, of many genes (29). ACh and nicotine are known to increase TH expression and, consequently, CAT synthesis in AGCCs. These two molecules similarly bind to nicotinic and muscarinic acetylcholine receptors (nAChRs and mAChRs, respectively). We used nicotine *in lieu* of ACh in this and the rest of the experiments to stimulate AGCCs, as nicotine is more stable for storage and in culture medium. According to EMSAs, AP-1 binding to the AP-1-binding sequence in the 5′ upstream region of the *Egr1* gene was reduced with nuclear extracts of AGCCs from male *Ephb6* KO mice compared with those from WT counterparts (Fig. 4*A*). We confirmed that the shifted AP-1 bands in EMSA contained both c-Jun and c-Fos (Fig. S1, *A* and *B*). AP-1 is a dimer of Jun and Fos family members, and c-Jun is the major subtype of Jun proteins. Nicotine-triggered c-Jun phosphorylation was compromised in male *Ephb6* KO AGCCs compared with the WT counterparts (Fig. 4*B*).

Compromised signaling pathways upstream of c-Jun in male Ephb6 KO AGCCs

We assessed the activation status of signaling molecules upstream of c-Jun. The results indicated reduced JNK phosphorylation at Thr^{173}/Tyr^{185} (Fig. 5*A*) and also MKK7 phosphorylation at Ser^{227}/Thr^{275} (Fig. 5*B*) in male KO AGCCs stimulated by nicotine. In these cells, G-LISA assay revealed reduced activation of the signaling molecule RAC1 farther upstream (Fig. 5*C*).

Using inhibitors of JNK, MKK7, and RAC1 and employing *Egr1* mRNA expression as a readout, we revealed that suppression of these signaling molecules could indeed repress *Egr1* expression in AGCCs from WT male mice (Fig. 5, *D–F*, *left panels*), demonstrating the relevance of the reduced activity of these molecules in male KO AGCCs to decreased *Egr1* expression. On the other hand, these inhibitors had no effect on mRNA expression of an unrelated molecule, *Cbl* (Fig. 5, *D–F*, right panels), indicating that the effect of these inhibitors on *Egr1* expression was not due to general toxicity.

On the other hand, activation of ELK1, ERK1/2, and p38MAPK, which could theoretically promote *Egr1* expression, was not changed in male KO AGCCs compared with their WT counterparts (Fig. 6, *A–C*).

EPH/EFN signaling direction and the role of testosterone

We assessed the signaling direction between EPHB6 and EFNBs by using a solid-phase anti-EPHB6 Ab (for forward signaling) and EPHB6-Fc (for reverse signaling). As shown in Fig. 7*A*, when tsAM5NE chromaffin cells were cultured on EPHB6-Fc– but not anti-EPHB6 Ab– coated wells, their nicotine-stimulated TH level was augmented, suggesting that reverse signaling from EPHB6 to EFNBs enhances TH synthesis.

EPHB6 can interact with EFNB1, EFNB2, and EFNB3. We investigated which one was essential for reverse signaling. Because EFNB3 KO in mice manifested no CAT secretion phenotype (20), we focused on EFNB1 and EFNB2. As shown in Fig. 7*B*, the solid-phase anti-EFNB1 Ab but not the anti-EFNB2 Ab augmented nicotine-stimulated TH expression in tsAM5NE chromaffin cells (Fig. 7*B*), suggesting that EPHB6's effect on CAT synthesis is mainly via EFNB1 reverse signaling.

To clarify the role of testosterone in reducing CAT synthesis in AGCCs from male KO mice, we cultured AGCCs from female KO mice in the presence or absence of testosterone. As shown in Fig. 7*C*, cell membrane–impenetrable BSA-conjugated testosterone caused lower CAT content in AGCCs from KO but not WT female mice. This indicates that the nongenomic effect of testosterone, but not the simple presence of testicles in adult life or during fetal development, is responsible for the observed diminished AGCC CAT biosynthesis in male KO mice.

Discussion

Our previous study showed that EPHB6 is highly expressed in the medullae of the adrenal gland and that *Ephb6* KO leads to reduced 24-h urine CAT levels (16). We further demonstrated that EPHB6 is critical for regulating AGCC ion channel opening and, consequently, for controlling acute CAT secretion (23). The acute secretion of CAT from AGCCs is from a stored, immediately releasable pool of CAT-containing vesicles docked near the cell membrane (30). Long-term secretion of CAT, caused by repeated stimulation of AGCC acetylcholine, involves recruitment of vesicles from the reserve pool (31). The 24-h urine CAT levels reflect the sum of both acute and long-

Figure 1. Epinephrine content and TH expression in the adrenal glands of WT and KO mice. *A*, total epinephrine content in the adrenal glands of WT and KO mice. The results from three independent experiments using different mice were pooled, and the results are shown as means + S.D. with data points. The data were analyzed by two-way paired Student's *t* test, and the significant *p* value is indicated. *B*, similar sizes of KO and WT adrenal glands. Adrenal glands were serially sectioned at an interval of 50 μm at 5-μm thickness. Representative micrographs of the largest HE-stained transection of the gland from each group are presented. The total volume of the adrenal gland medulla was determined by following formula: size of the medulla = mean area of all sections that contains the medulla × length of the medulla. The results from three individual medullae from different mice of each group were pooled, and the results are shown as means + S.D. with data points. No significant difference between KO and their WT counterparts was found (two-way paired Student's *t* test). *C*, TH mRNA expression in adrenal gland medullae of KO and WT mice. Total RNA was extracted from adrenal medullae. The TH mRNA level was analyzed by RT-qPCR. β-Actin levels were used as internal controls. Samples were measured in triplicate, and the data from three independent experiments using different mice were pooled and expressed as graphs of TH signal/β-actin signal ratios (means + S.D. with data points). The significant *p* value (two-way paired Student's *t* tests) is indicated. *D*, TH protein expression in the adrenal medullae of KO and WT mice. TH protein levels in the adrenal gland medullae were analyzed by immunoblotting. Representative immunoblotting images are shown. The signal ratios of TH *versus* β-actin were quantified by densitometry. Densitometry data from three or more (as indicated) independent experiments using different mice were pooled and are presented as graphs (means + S.D. with data points). The significant *p* value (two-way paired Student's *t* tests) is indicated.

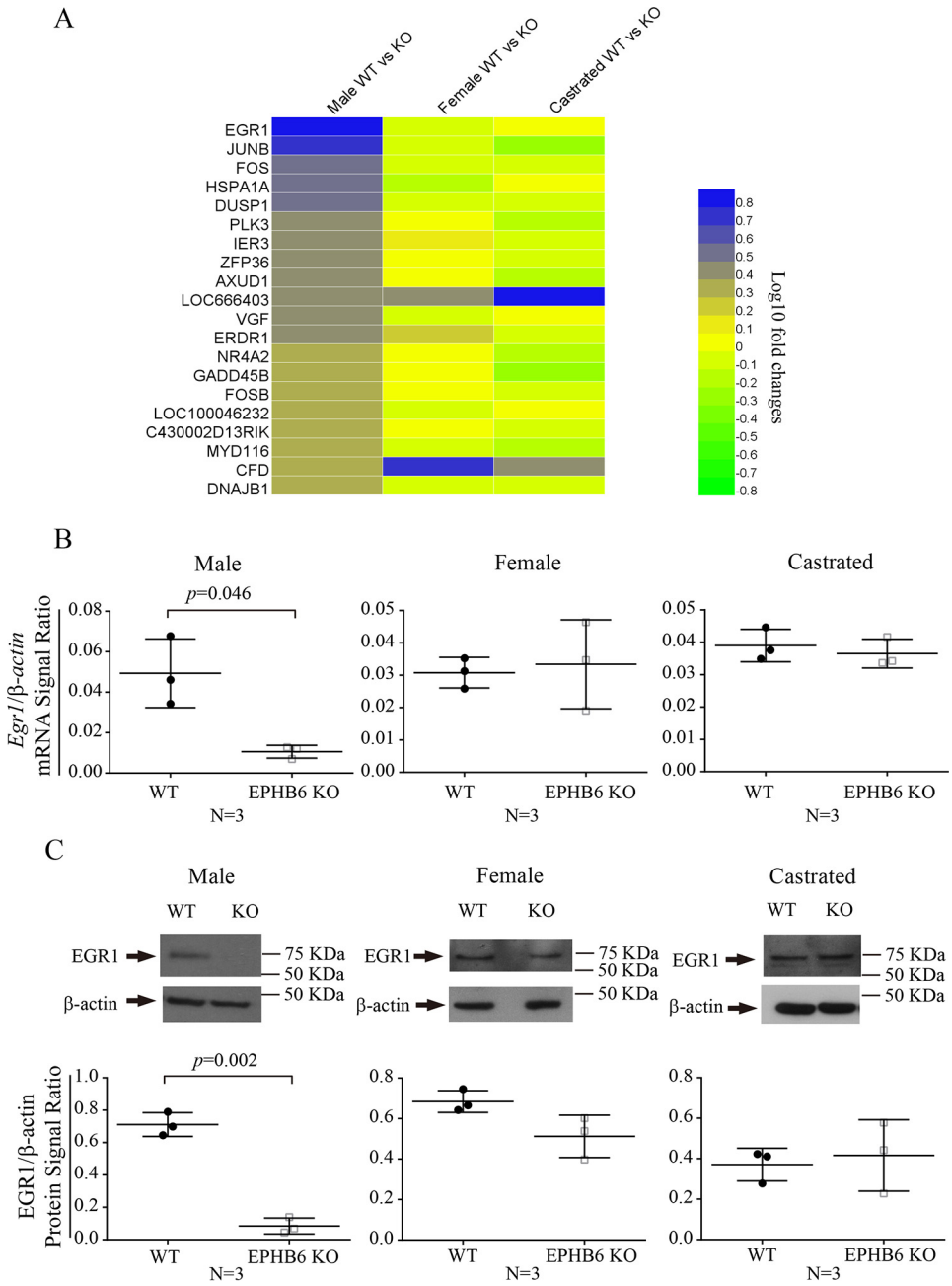

Figure 2. Identification of reduced Egr1 expression in the adrenal glands of male KO mice. *A*, significantly altered expression of genes in the cRNA microarray analysis of adrenal gland medullae from KO mice and the WT. Total RNA was extracted from adrenal glands and subjected to cRNA microarray analysis. Three biological replicates using difference mice for each group were employed, and mean signal levels of each gene in each group were calculated. Genes whose mean signal levels differed more than 2-fold between male WT and male KO groups were selected, and the ratios of their mean signal levels are presented in the *left column* of a $\log_{10}$-scaled heatmap. The ratios of the mean signal levels of these selected genes for female WT *versus* female KO groups are presented in the *center column*, whereas those between castrated WT males *versus* castrated KO males are presented in the *right column*. *B*, reduced expression of Egr1 mRNA in adrenal medullae from male KO mice. *Egr1* mRNA levels in the adrenal gland medullae were analyzed by RT-qPCR. β-Actin levels were used as internal controls. Samples in RT-qPCR were in triplicate, and *Egr1*/β-actin signal ratios from three independent experiments using different mice were pooled and expressed as means + S.D. with data points. The significant *p* value (two-way paired Student's *t* tests) is indicated. *C*, reduced Egr1 protein expression in the adrenal medullae of male EPHB6 KO mice. EGR1 protein levels of adrenal gland medullae were analyzed by immunoblotting, and representative images are shown. The intensity of the EGR1 and β-actin bands was measured by densitometry. The results of three independent experiments using different mice were pooled, and the signal ratios of EGR1 *versus* β-actin are presented as graphs (means + S.D. with data points). The significant *p* value (two-way paired Student's *t* tests) is indicated.

term CAT secretion. CAT biosynthesis might affect both of these processes by controlling their respective pool sizes. To assess this, we examined the CAT content of adrenal glands from KO mice. Even though the size of the glands and their medullae from male and female KO mice was similar to their WT and castrated male KO counterparts, the epinephrine content of the adrenal gland medullae from male KO mice was significantly lower compared with the WT counterparts. This suggests that CAT biosynthesis and/or degradation in the male KO adrenal gland is abnormal.

TH is the rate-limiting enzyme in CAT biosynthesis (32). The reduced TH levels in KO AGCCs likely led to the lowered

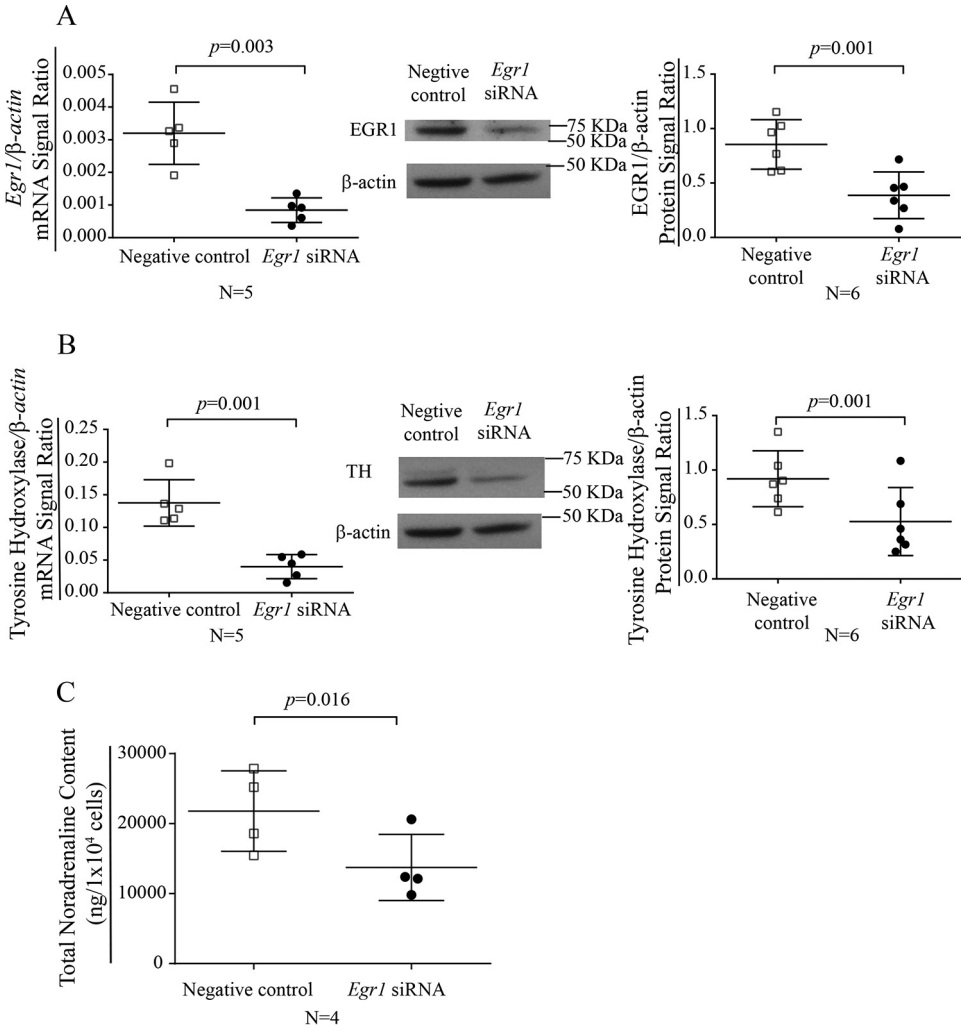

Figure 3. Egr1 knockdown by siRNA reduces TH expression and the epinephrine content of the chromaffin cell line tsAM5NE. *Egr1* siRNA and negative control *siRNA* were transfected into the adrenal gland chromaffin cell line tsAM5NE. *A*, reduced expression of Egr1 in tsAM5NE cells after Egr1 knockdown. The cells were harvested 24 h after *Egr1* and control siRNA transfection, and the *Egr1* mRNA (*left panel*) and protein (*right panel*) levels were determined by RT-qPCR and immunoblotting, respectively. Data from five or more (as indicated) independent experiments were pooled and presented as means + S.D. with data points of the ratios of *Egr1* mRNA signal *versus* β-*actin* mRNA signal and ratios of EGR1 protein signal *versus* β-actin protein signal. *p* values are indicated (two-way paired Student's *t* tests). *B*, TH expression was reduced in tsAM5NE cells after Egr1 knockdown. tsAM5NE cells were harvested 72 h after *Egr1* siRNA transfection, and the TH mRNA (*left panel*) and protein (*right panel*) levels were determined by RT-qPCR and immunoblotting, respectively. Data from five or more (as indicated) independent experiments were pooled and are presented as means + S.D. with data points of the ratios of TH mRNA signal *versus* β-actin mRNA signal and ratios of the TH protein signal *versus* β-actin protein signal. The *p* values are indicated (two-way paired Student's *t* tests). The same membranes were first blotted with anti-EGR1 Ab and then stripped and reblotted with anti-TH Ab and anti-β-actin Ab, so the same β-actin immunoblotting was used as loading controls for both *A* and *B*. *C*, reduced noradrenaline content in tsAM5NE chromaffin cells after Egr1 knockdown. tsAM5NE cells were harvested and then lysed 72 h after *Egr1* siRNA transfection. Noradrenaline levels in the cleared supernatants were determined by noradrenaline ELISA, in which samples were measured in duplicate. Results from four independent experiments were pooled and presented as means + S.D. with data points. The *p* value is indicated (two-way paired Student's *t* tests).

CAT biosynthesis in these KO cells. TH activity in AGCCs is regulated by phosphorylation of its serine residues and by its protein level. Its Ser^{31} phosphorylation augments its activity, whereas Ser^{40} and Ser^{19} phosphorylation alleviates feedback inhibition (33). Examination of TH phosphorylation at Ser^{31}, Ser^{40}, and Ser^{19} in adrenal glands from male KO mice without or with nicotine stimulation revealed no consistent differences compared with the WT counterparts (data not shown). However, TH protein and mRNA levels were reduced in male KO adrenal glands, indicating reduced transcription from the TH gene.

To elucidate the mechanisms by which EPHB6 regulates TH gene transcription, we profiled the transcriptome of adrenal glands from male, female, and castrated KO and WT mice. We confirmed by RT-qPCR and immunoblotting that the expression of the top hit *Egr1*/EGR1 was decreased in the adrenal gland medullae of male KO mice and that such a change disappeared after castration, agreeing well with the phenotype of TH expression and CAT content of KO adrenal glands. EGR1 is a zinc-finger protein belonging to the EGR family of transcription factors (34). It activates the genes containing EGR1-binding sites. We searched a 300-bp 5′ upstream sequence of the mouse (C57BL/6) TH gene with the transcription factor-finding program AliBaba2.1 and found two EGR1-binding sites at −41/−50 and −112/−121 (the first nucleotide before the TH gene is designated as position −1) (Fig. 8). siRNA knockdown of EGR1 in AGCCs led to reduced TH expression at both mRNA and protein levels, with concurrent reduction of norepineph-

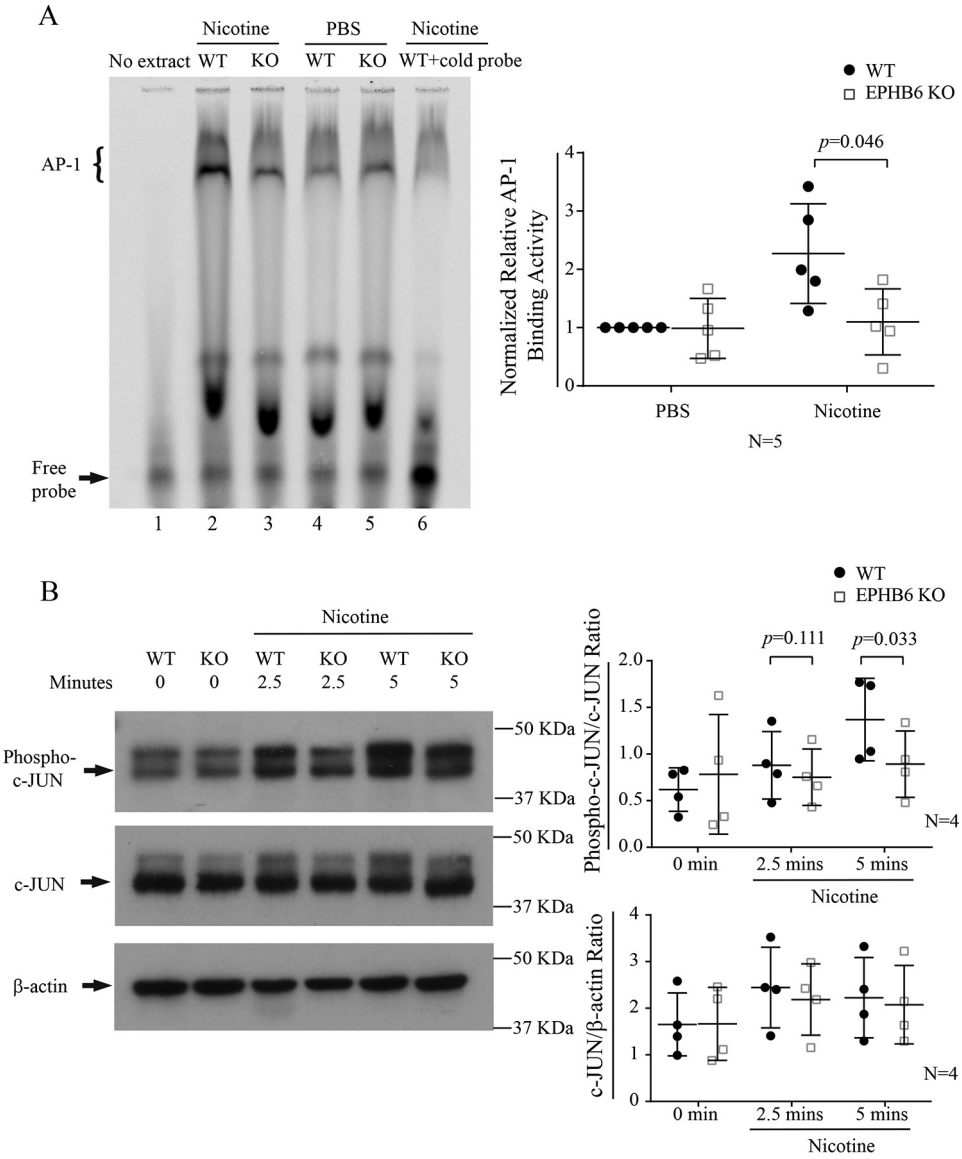

Figure 4. AP-1 level and c-Jun activation in KO and WT adrenal gland medullae. *A*, decreased AP-1 association with its binding site in the *Egr1* gene in AGCCs of male Ephb6 KO mice. The binding of AP-1 of AGCCs with the AP-1–binding site in the *Egr-1* gene enhancer was analyzed by EMSA. A representative image is shown (*left panel*). The shifted AP-1 bands in the assay are indicated by the *bracket*. *Lane 1*, no nuclear protein was added; *lanes 2–5*, 10 μg of nuclear protein from WT or KO adrenal gland medullae was added to the reaction; *lane 6*, a 200-fold molar excess of unlabeled probe as competitor was added to the reaction to determine the background of the AP-1 binding. The signals of the shifted AP-1 bands were quantified by densitometry. The specific AP-1 binding signal of each sample was determined by the intensity of the shifted AP-1 band minus the background signal of that region in *lane 6*. The results were normalized to determine normalized relative AP-1–binding activity (specific AP-1 binding signal of a test sample/specific AP-1 binding signal of WT AGCCs stimulated with PBS). Results of five independent experiments using different mice were pooled, and the normalized relative AP-1 binding signals (means + S.D. with data points) are presented in a graph (*right panel*). The significant *p* value is shown (two-way paired Student's *t* test). *B*, decreased c-Jun phosphorylation in adrenal medullae from male EPHB6 KO mice. Adrenal medullae from male KO and WT mice were isolated and cultured for 2 h. They were then lysed at 0, 2.5, and 5 min after nicotine (20 μM) stimulation. Nuclear proteins from the medullae were extracted. Total and phosphorylated c-Jun levels in the nuclear proteins were determined by immunoblotting. Four independent experiments were conducted. Representative immunoblotting images are shown (*left panel*). The signals were quantified by densitometry. The signal ratios of phosphorylated *versus* total c-Jun and total c-Jun *versus* β-actin of four independent experiments using different mice were pooled and are presented as graphs (means + S.D. with data points, *right panels*). Significant *p* values are indicated (two-way paired Student's *t* tests).

rine content in the AGCCs, proving that EGR1 indeed positively regulates TH expression. In support of our conclusion, Papanikolaou and Sabban (34) reported that, in the 5′ upstream sequence of the rat TH gene from positions −122 to −114, there is an EGR1-binding site, CACCCCCGC, which is proven to positively regulate TH transcription in a reporter assay. This rat EGR1-binding sequence is identical to another *EGR1*-binding site in the mouse TH gene between positions −103 and −95 (CACCCCCGC). Our current EGR1 expression and knockdown results established the correlation between EGR1 expression levels and CAT biosynthesis.

The reduced *Egr1* mRNA levels in KO AGCCs suggested that *EPHB6* deletion decreased *Egr1* transcription. In the 5′ UTR of the first exon of the mouse *Egr1* gene, there is an AP-1 binding site (ACTGACCTAGA) between positions +383 and +393 (the first nucleotide in exon 1 is designated as position +1; the start codon is at position +1667) (Fig. 8). This site has been proven to be functional in enhancing *Egr1* transcription in a

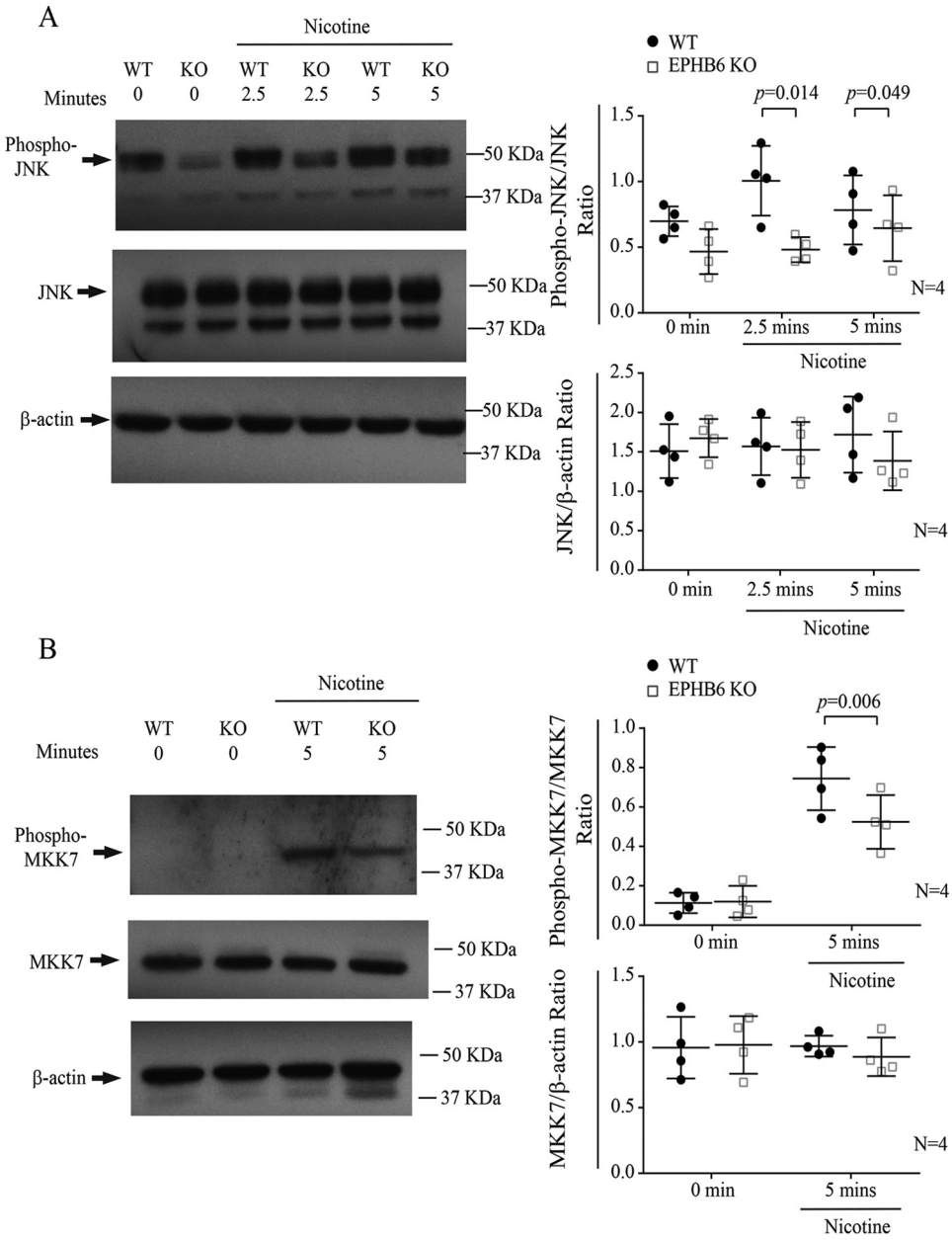

Figure 5. EPHB6 signaling pathway upstream of c-Jun. *A*, decreased MKK7 phosphorylation in adrenal medullae from male EPHB6 KO mice after nicotine stimulation. *B*, decreased JNK phosphorylation in adrenal medullae from male EPHB6 KO mice after nicotine stimulation. For *A* and *B*, adrenal medullae from male KO and WT mice were prepared as described in Fig. 4*B*. They were then lysed at 0, 2.5, and 5 min after nicotine (20 μM) stimulation. Total and phosphorylated MKK7 and JNK in the lysates were analyzed by immunoblotting. Representative immunoblotting images are shown (*left panels*). The signals were quantified by densitometry, and the signal ratios of phospho-MKK7 *versus* total MKK7, total MKK7 *versus* β-actin, phospho-JNK *versus* total JNK, and total JNK *versus* β-actin from four independent experiments using difference mice were pooled and are presented as graphs (means + S.D. with data points, *right panels*). Significant *p* values are indicated (two-way paired Student's *t* tests). *C*, male KO adrenal gland medullae presented reduced RAC1 activity. The adrenal gland medullae were stimulated with nicotine (20 μM) at 37 °C for 0 and 2.5 min. Activated RAC1 in the tissue was extracted and quantified by a RAC1 G-LISA kit. Samples were assayed in duplicate. Three independent experiments using different mice were performed, and the results were normalized according to the following formula: normalized RAC1 activity = RAC1 activity of a sample/RAC1 activity of WT medulla at 0 min. Means + S.D. with data points of the normalized RAC1 activity of the three independent experiments are shown. The significant *p* value is indicated (two-way paired Student's *t* test). *D*--*F*. JNK, MKK7, and RAC1 inhibitors repressed Egr1 mRNA expression in WT adrenal gland medullae. Adrenal gland medullae were isolated from WT male mice. They were cultured in the presence of JNK inhibitor (25 μM), MKK7 inhibitor (50 μM), or RAC1 inhibitor (50 μM) for 4 h at 37 °C. Total RNA from the adrenal gland medullae were isolated, and *Egr1*, *β-actin*, and *Cbl* mRNA transcripts were amplified by RT-PCR. Three or more (as indicated) independent experiments using different mice were conducted. The pooled data from these experiments were expressed as means + S.D. with data points of signal ratios of target RNA/*β-actin* mRNA. The significant *p* values are indicated (two-way paired Student's *t* test).

reporter gene assay in human HEK293 cells (36). Using an EMSA, we found that, in the *Ephb6* KO AGCCs, the AP-1-binding site in the *Egr1* gene had less association with the AP-1 transcription factor compared with WT AGCCs. Our data established the correlation between active AP-1 binding and *Egr1* expression. Earlier literature showed that the reduced association of nuclear AP-1 with its binding of its target genes is correlated with the level of its target gene transcription (37, 38). There are other AP-1 binding sites in the mouse *Egr1* gene 5′ sequence (positions −153 to −144) and TH gene 5′ sequence

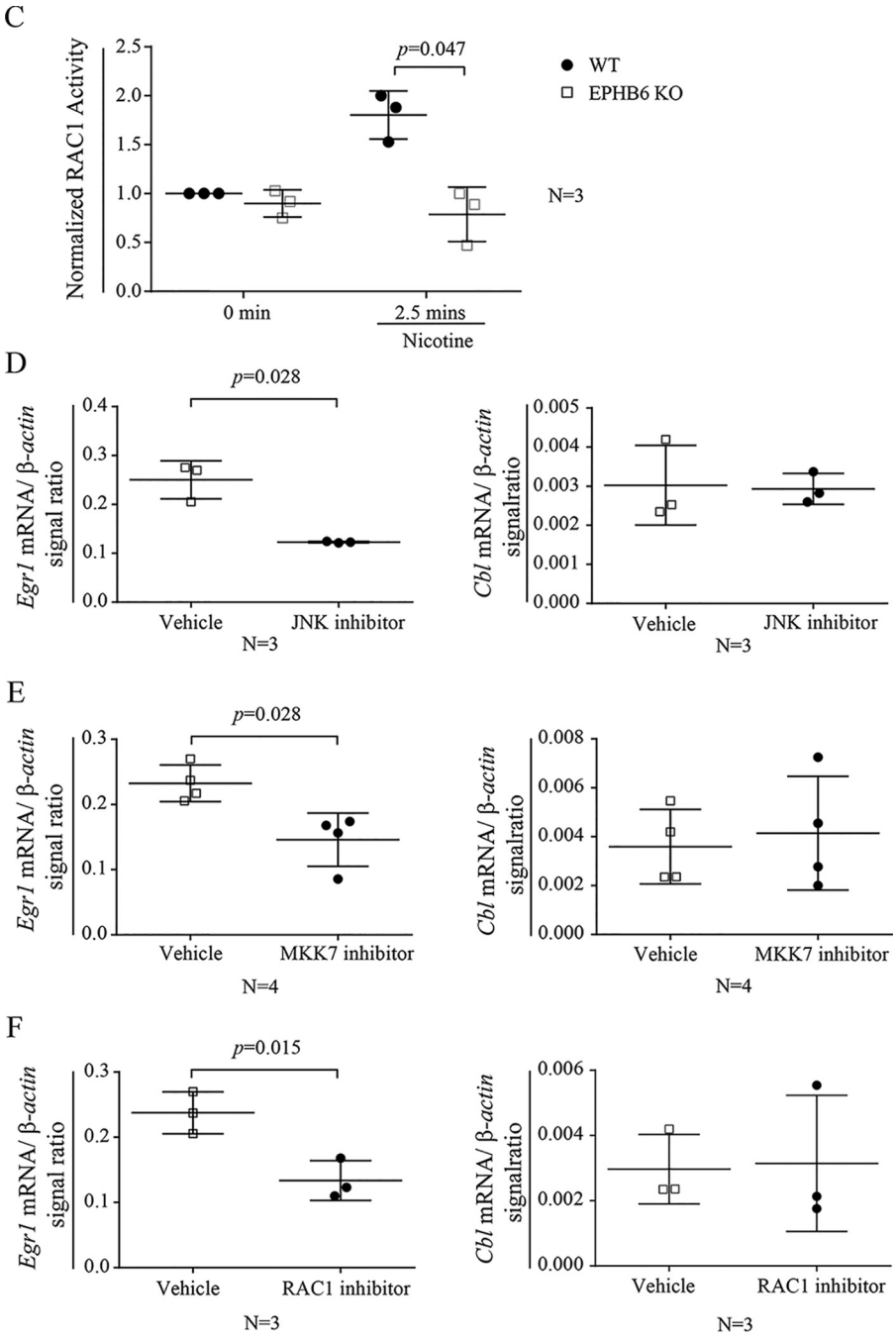

Figure 5—*Continued*

(positions −285 to −276). Conceivably, the enhancer activity of all of these AP-1-binding sites might be similarly affected by the reduced AP-1 association in the KO AGCCs, leading to diminished expression of *Egr1* and *TH* transcription sequentially or simultaneously.

AP-1 is a dimeric transcription factor composed of Jun and Fos family members. Jun proteins can form homodimers or form heterodimers with Fos proteins, both of which can associate with AP-1-binding sites, but Fos proteins can only bind to the AP-1 site via Jun proteins (39, 40). Heterodimeric c-Jun and c-Fos have high affinity for AP-1-binding sites in many genes (39). c-Jun Ser^{63} and Ser^{73} phosphorylation increases transcription of AP-1 target genes (41), although is not necessary for AP-1 nuclear import (42). We have shown that c-Jun S63 phosphorylation was reduced in male KO AGCCs.

JNK is responsible for c-Jun Ser^{63} and Ser^{73} phosphorylation (43). JNK is activated by dual phosphorylation at its Thr^{183}/Tyr^{185} in the kinase domain (43). MKK7 is the specific upstream kinase for such phosphorylation (44, 45) (Fig. 7). MKK7 itself is activated by phosphorylation at Ser^{271}, Thr^{275}, and Ser^{277} (46). Further upstream, the GTPase RAC1 controls MKK7 activation (47), although molecular details of how RAC1 affects MKK7 phosphorylation remain to be elucidated. We have demonstrated, as illustrated in Fig. 5, *A–C*, that activation of all key molecules in this signaling pathway, *i.e.* JNK, MKK7, and RAC1, was compromised in male KO AGCCs. Further,

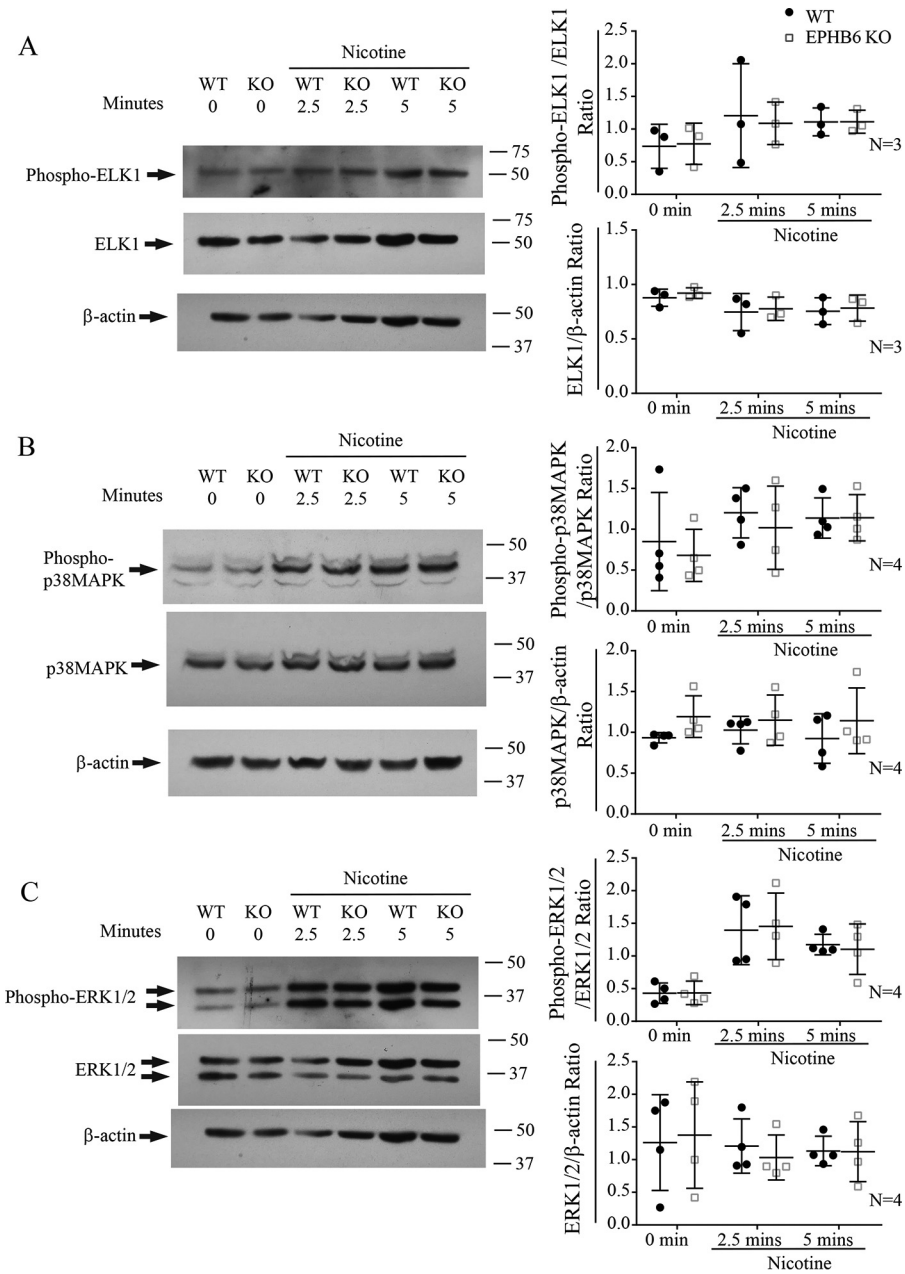

Figure 6. ERK1/2, p38MAPK, and ELK1 were not in the EPHB6 signaling pathway leading to CAT synthesis. *A–C*, nicotine-stimulated ERK1/2 (*A*), p38MAPK (*B*) and ELK1 (*C*) phosphorylation in adrenal medullae from male KO and WT mice were determined as described in Fig. 4*B*. Representative immunoblotting images are shown in the *left panels*. The intensity of the bands was measured by densitometry. The results of three or more (as indicated) independent experiments using different mice were pooled, and the signal ratios of phospho-ERK1/2 *versus* total ERK1/2, total ERK1/2 *versus* β-actin, phospho-p38MAPK *versus* total p38MAPK, total p38MAPK *versus* β-actin, phospho-ELK1 *versus* total ELK1, and total ELK1 *versus* β-actin of KO and WT medullae are presented as graphs (means + S.D. with data points). No significant differences between KO and WT medullae were found (two-way paired Student's *t* tests). The same membranes were sequentially blotted with anti-phospho-ELK1, ELK1, phospho-ERK1/2, ERK1/2, and β-actin Abs, with a stripping process between these different immunoblottings. The same β-actin immunoblotting was used as a loading controls for both *A* and *C*.

inhibitors of these signaling molecules repressed *Egr1* expression (Fig. 5, *D–F*), as expected, demonstrating the relevance of these molecules for *Egr1* expression. As *Egr1* knockdown led to decreased TH expression, the relevance of these molecules for final CAT synthesis is also suggested.

We investigated the signaling events further upstream, where EPHB6 on the surface interacts with its cell surface ligand EFNs. As reviewed in the introduction, multiple EFN ligands can bind an EPH and trigger forward signaling. In the case of EPHB6, it has three potential ligands: EFNB1, EFNB2, and EFNB3. These ligands can also function as receptors, receive stimulation from EPHB6, and conduct reverse signaling into the cells. To mimic forward signaling from cell surface EFNBs to cell surface EPHB6, we coated wells with anti-EPHB6 Ab. Use of the anti-EPHB6 Ab provides specific stimulation to EPHB6 but not to other EPHs with which EFNBs could also interact. Such treatment did not augment nicotine-stimulated TH expression (Fig. 7*A*), suggesting that the forward signaling

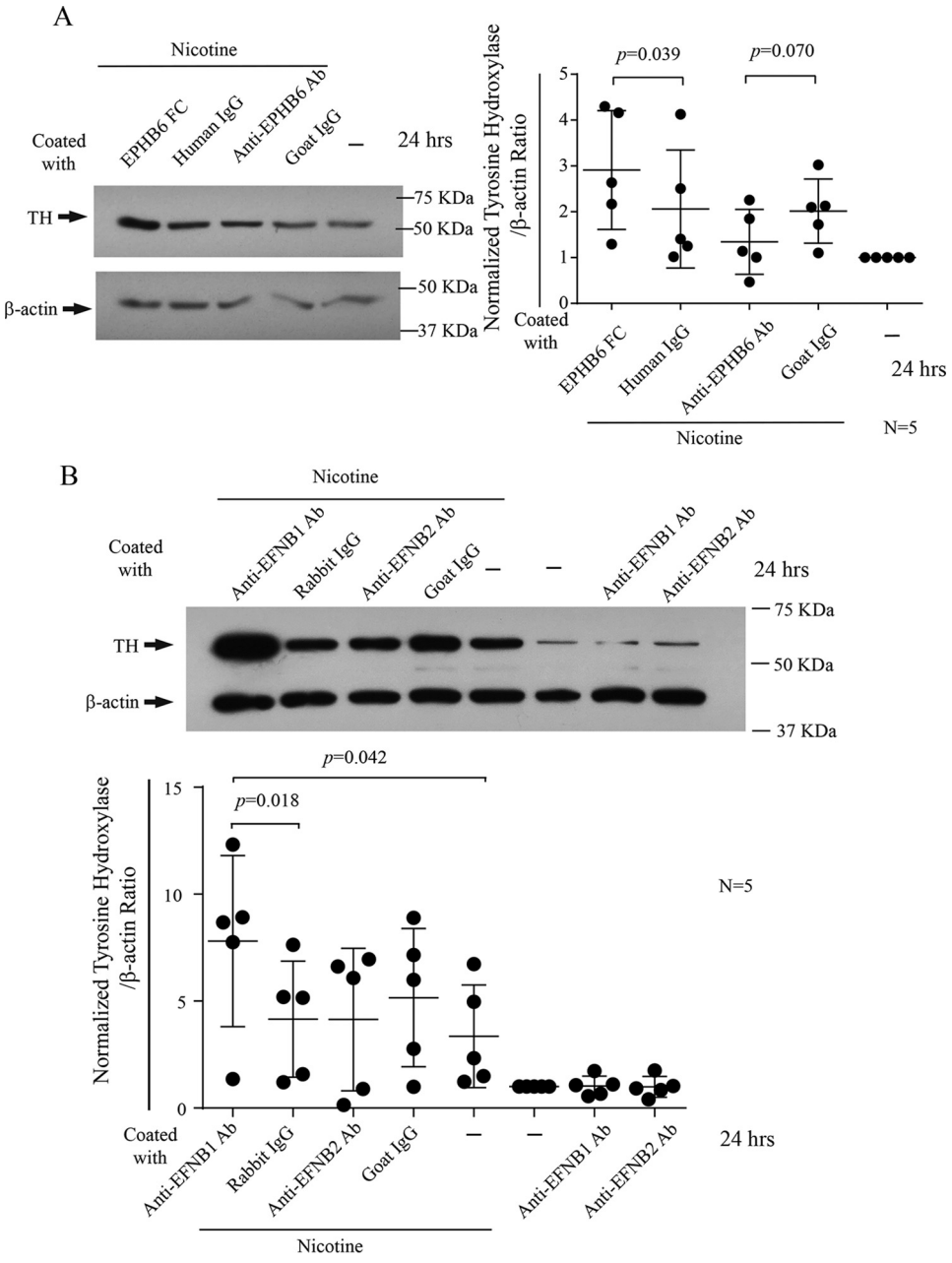

Figure 7. EPH/EFN signaling direction and the role of testosterone. *A*, reverse but not forward signaling between EPHB6 and EFNBs promotes TH protein expression upon nicotine stimulation. tsAM5NE chromaffin cells were cultured in 24-well plates coated with anti-EPHB6 Ab, normal goat IgG, recombinant EPHB6-Fc, or normal human IgG (2 μg/ml for coating) for 24 h. They were lysed 4 h after nicotine (40 μM) stimulation at 33 °C. TH protein levels of the cells were determined by immunoblotting. β-Actin was used as loading control. Five independent experiments were performed, and a representative immunoblot is shown (*left panel*). The signals of the immunoblots were determined by densitometry. The results were normalized using the following formula: normalized TH protein expression = ratio of TH/β-actin of cells cultured in different coated wells/ratio of TH/β-actin of cells cultured in wells without any coating. The normalized TH protein expression levels of the five experiments were pooled, and their means + S.D. with data points are presented as a graph (*right panel*). Significant *p* values are indicated (two-way paired Student's *t* tests). *B*, EFNB1, but not EFNB2, promotes TH protein expression in tsAM5NE chromaffin cells upon nicotine stimulation. The experiments were carried out, and the results are presented as described in *A*, except that the wells were coated with anti-EFNB1 Ab, normal rabbit IgG, goat anti-EFNB2 Ab, or normal goat IgG (2 μg/ml for coating) for 24 h. Normalized TH protein expression levels of five experiments were pooled, and their means + S.D. with data points are presented as a graph (*bottom panel*). Significant *p* values are indicated (one-way paired Student's *t* tests). *C*, nongenomic effect of testosterone on norepinephrine synthesis in AGCCs from female EPHB6 KO and WT mice. Mouse AGCCs were isolated from female EPHB6 KO and WT mice and cultured in DMEM containing 15% (v/v) FCS (10,000 cells per well). The cells were pretreated with cell membrane–impermeable, BSA-conjugated testosterone (1.1 μg/ml; *Testo-BSA*) or BSA for 15 min. Nicotine (20 μM) was then added to the culture. The cells were cultured for 16 h at 37 °C and harvested. They were lysed, and norepinephrine levels in the cleared lysates were measured by ELISA. Samples were assayed in duplicate. Norepinephrine content per cell were calculated based on the cell number per well and the amount of norepinephrine detected in the lysate of all the cells in a well. The means + S.D. with data points of norepinephrine levels per cells of three independent experiments were pooled and are presented. Significant *p* values are indicated (two-way Student's *t* test).

is not relevant. To mimic the reverse signaling from cell surface EPHB6 to cell surface EFNBs, we coated recombinant human IgG Fc-conjugated EPHB6 (EPHB-Fc) on the wells, and such solid-phase EPHB6 could enhance the elevated TH expression stimulated by nicotine. This indicates that the reverse signaling from EPHB6 to EFNBs is responsible for the observed AGCC

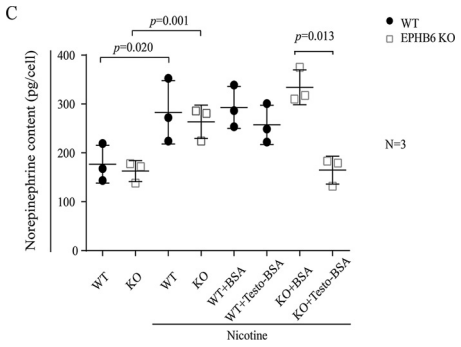

Figure 7—*Continued*

phenotype. To further dissect the reverse signaling pathway, we coated anti-EFNB1 and anti-EFNB2 Abs on the wells to initiate specific reverse signaling through these molecules and identified EFNB1 as the essential one (Fig. 7*B*). As our early study has already determined that EFNB3 KO does not cause any AGCC phenotype, we concluded that the EPHB6-to-EFNB reverse signaling in AGCCs is via EFNB1. It is well known that EFNBs co-localize with and activate RHO family GTPases, including RAC1, in many different types of cells (48–50). Thus, a putative signaling pathway starting from EPHB6 to EFNB1/RAC1/MKK7/JNK/c-Jun/AP-1/EGR1/TH/CAT is suggested.

The pathway postulated above was active when the AGCCs were stimulated with the AChR agonist nicotine, which binds to nAChR and mAChR, similar to acetylcholine. The major consequence of nAChR and mAChR activation by nicotine or ACh is the change of cytosolic cation concentration. This leads to larger Ca^{2+} influx through voltage-gated calcium channels (VGCCs). The increased Ca^{2+} concentration induces a cascade of downstream signaling events. These events include the activation of RAC1/MKK7/JNK/c-Jun-AP1, as demonstrated in our experiments using WT AGCCs (Figs. 4 and 5). The details of the signaling between Ca^{2+} and RAC1 remain to be further elucidated. Obviously, the EFNB1 reverse signaling pathway overlaps with the AChR signaling pathway starting from RAC1 in the RAC1/MKK7/JNK/c-Jun-AP1 cascade (Fig. 8) and is needed for the optimal function of the latter, as deletion of EPHB6 (the stimulator of EFNB1) caused compromised strength of this RAC1/MKK7/JNK/c-Jun-AP1 pathway, leading to decreased CAT synthesis.

We conducted an additional experiment to show that the nongenomic effect of testosterone was responsible for suppressed CAT synthesis in KO AGCCs. In this experiment, AGCCs from female KO mice were treated with testosterone. The use of female mice guaranteed a lack of exposure of AGCCs to high levels of testosterone *in vivo*. Although AGCCs from female KO mice in the absence of exogenous testosterone had no phenotype with regard to *Egr1* expression, the testosterone treatment rendered them a phenotype similar to that seen in male KO AGCCs. This suggests that the presence of testosterone in adult life, but not during fetal development, is responsible for its action in concert with EPHB6 in leading to the *Egr1* phenotype and, consequently, the CAT phenotype.

Our previous publication (23) suggests that the nongenomic effect of testosterone is responsible for promoting outward K^+ efflux and, hence, earlier closure of VGCCs. We hypothesize that, under normal circumstances, EFNB1 has a suppressive effect on testosterone's K^+ efflux-promoting effect, as illustrated in Fig. 8. In the absence of EFNB1, such a suppressive effect is released. This results in larger K^+ efflux and earlier termination of the Ca^{2+} surge, leading to a lower strength of the RAC1/MKK7/JNK/c-Jun/AP-1 signaling pathway. In such a way, EFNB1, nAChR, and cell surface testosterone receptor signaling pathways interact among themselves. The sum of their effect determines the outcome of CAT synthesis (Fig. 8).

In the 5′ upstream region of the *Egr1* gene, there are two groups of serum-responsive elements (SREs). The proximal group has two SREs at positions +1278/+1295 and +1300/+1313, and the distal group has three SREs at positions +974/+992, +1025/+1042, and +1045/+1059 (34). Depending on the cell type, either of the SRE groups has been shown to enhance *Egr1* transcription (36, 51). ELK1 associates with serum-responsive factors, and the complex binds to SREs of target genes to enhance their transcription (52). ELK1 phosphorylation at Ser^{383} and Ser^{389} leads to its de-SUMOylation and allows its nuclear translocation and activation (53, 54). ERK2 and p38MAPK are the upstream kinases responsible for such phosphorylation (35). We found no difference in the activation of ELK1, ERK2, and p38MAPK based on their phosphorylation, suggesting that the pathway ERK2 > p38MAPK > ELK1 > SRE in *Egr1* transcriptional regulation is not involved in the EPHB6-mediated phenotype in AGCCs with regard to catecholamine biosynthesis (Fig. 8).

In summary, with the results of this study, we could construct a hypothetic pathway of EPHB6 > EFNB1 > RAC1 > MKK7 > JNK > c-Jun/AP1 > EGR1 > TH > CAT, delineating the regulation of CAT biosynthesis by EPHB6, as shown in Fig. 8. This pathway merges with the signaling pathway of AChR > Ca^{2+} > RAC1 > MKK7 > JNK > c-Jun/AP1 > EGR1 > TH > CAT starting from RAC1 and is necessary for optimal function of the latter. Deletion of EPHB6 (hence, diminished reverse signaling via EFNB1) compromises this signaling pathway, resulting in decreased CAT biosynthesis. The default nongenomic effect of testosterone is to augment K^+ outflow via the BK channel, leading to a faster closure of VGCC and, hence, lower total Ca^{2+} influx triggered by ACh. EFNB1 reverse signaling negatively regulates such a testosterone effect. In the absence of EPHB6 (hence, reduced EFNB1 reverse signaling), the augmenting effect of testosterone on K^+ efflux is now revealed, leading to faster VGCC closure and resulting in a negative effect on the Ca^{2+} > RAC1 > MKK7 > JNK > c-Jun/AP1 > EGR1 > TH > CAT pathway.

In addition to enhancing our knowledge in the area of chromaffin cell biology, the elucidation of this signaling pathway from EPHB6 to CAT and the interactions among EPHB6, AChR, and testosterone in this study could provide us with potential drug targets for regulating catecholamine biosynthesis, which is implicated in normal and pathological conditions such as blood pressure regulation and Parkinson's disease. In future studies, gaps in the signaling pathways between EFNB1 and RAC1, between RAC1 and MKK7, and between EFNB1 and cell surface androgen receptors need to be investigated further.

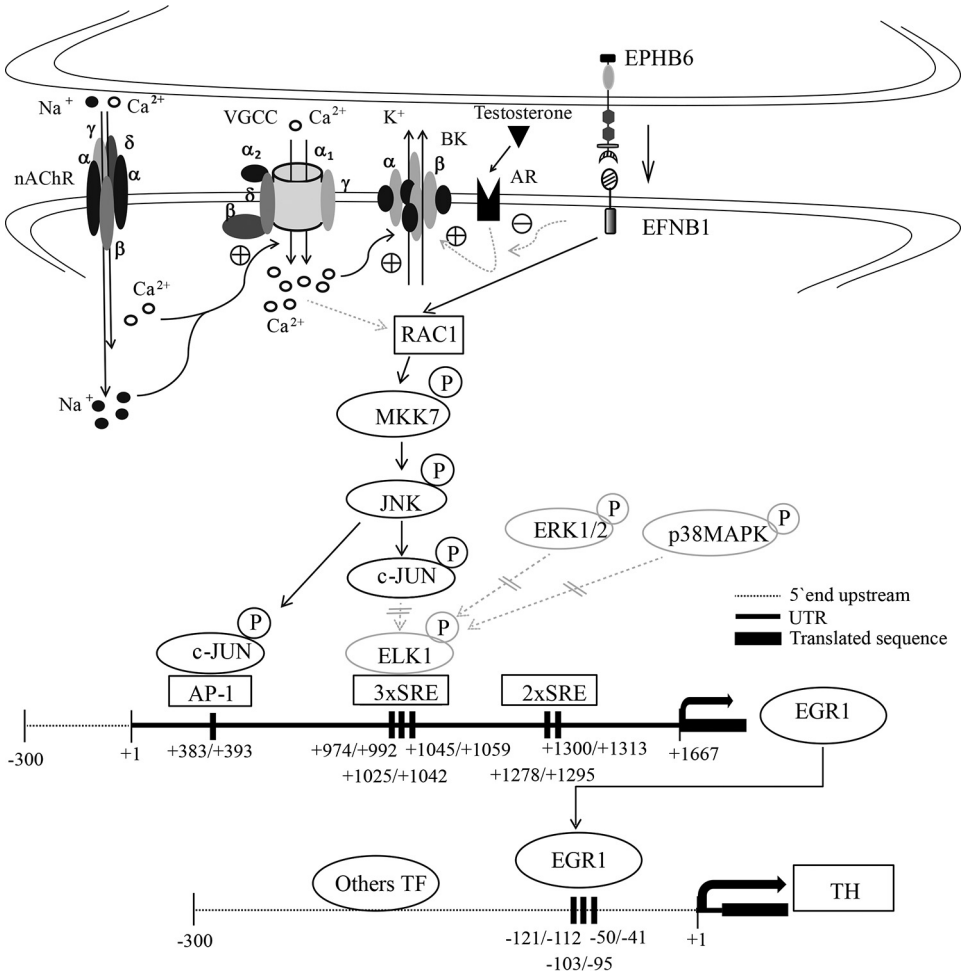

Figure 8. A model of the signaling pathway from EPHB6 to catecholamine biosynthesis in AGCCs. This diagram illustrates a hypothetic pathway from cell surface EPHB6 to CAT biosynthesis in AGCCs. EPHB6 exerts reverse signaling through EFNB1, which transduces signals into AGCCs and activates RAC1. RAC1, in turn, activates MKK7. MKK7 phosphorylates and activates JNK, which further phosphorylates c-Jun. c-Jun phosphorylation leads to increased nuclear AP-1 association with the AP-1 site in the 5′ UTR (+ 383/+393) of the *Egr1* gene. This augments *Egr1* expression at both the mRNA and protein levels. EGR1 binds to three EGR1-binding sites in the 5′ upstream sequence of the *TH* gene at −121/−112, −103/−96, and −50/−41 and augments transcription and translation of TH, the rate-limiting enzyme in CAT biosynthesis. This pathway merges with the signaling pathway of AChR > Ca^{2+} > RAC1 > MKK7 > JNK > c-Jun/AP1 > EGR1 > TH > CAT starting from RAC1 and is necessary for optimal function of the latter. Deletion of EPHB6 (hence, diminished reverse signaling via EFNB1) compromises this signaling pathway, resulting in decreased CAT biosynthesis. The default nongenomic effect of testosterone is to augment K^+ outflow via the BK channel, leading to a faster closure of VGCCs and, hence, lower total Ca^{2+} influx triggered by ACh. EFNB1 reverse signaling negatively regulates such a testosterone effect. In the absence of EPHB6 (hence, reduced EFNB1 reverse signaling), the augmenting effect of testosterone on K^+ efflux is now revealed, leading to faster VGCC closure and resulting in a negative effect on the Ca^{2+} > RAC1 > MKK7 > JNK > c-Jun/AP1 > EGR1 > TH > CAT pathway. On the other hand, although in the 5′ UTR of *Egr1* gene there are five SREs, they are not involved in the EPHB6 signaling pathway to TH biosynthesis because the activation of *ELK1*, which forms a complex with serum-responsive factors to become a transcription factor binding to SRE, and the activation of *ELK1* upstream kinases *ERK2* and *p38MAPK* are not affected by EPHB6 deletion. *Dark lines with arrows*, signaling proven in this study; *blocked gray lines with arrows*, theoretically possible signaling based on other studies but not functional in AGCCs according to our study; *solid dark lines with arrows*, signaling proven in this study; *dashed gray lines with arrows*, theoretically possible signaling based on other studies or hypothetical signaling pathways suggested by this study; *dashed gray lines with blockage signs*, theoretically possible signaling based on other studies but not functional according to our study; *TF*, transcription factor; *AR*, androgen receptor; *small open circles*, Na^+; *small solid circles*, Ca^{2+}; *large empty triangles*, testosterone.

Experimental procedures

Ephb6 gene KO mice

Ephb6 KO mice were generated in our laboratory as described previously (7). They were backcrossed to the C57BL/6 genetic background for more than 15 generations. Age- and gender-matched WT littermates served as controls. Experiments using castrated mice were conducted at least 3 weeks post-operation.

Epinephrine and norepinephrine assays

The adrenal glands were resected from *Ephb6* KO and WT mice or castrated KO mice and homogenized in 300 μl of 0.01 N HCl in the presence of 0.15 mM EDTA. Epinephrine levels in the cleared supernatants were determined by Epinephrine Research ELISA Kits (Rocky Mountain Diagnostics, Colorado Springs, CO; BAE-5100) according to the manufacturer's instructions. Cultured primary AGCCs were pretreated with cell membrane–impermeable BSA-conjugated testosterone (1.1 μg/ml, testosterone-3-(*O*-carboxymethyl)-oxime-BSA; testosterone-BSA; Aviva Systems Biology) or BSA for 15 min and then washed and stimulated with nicotine (20 μmol/liter) for 16 h at 37 °C. The cells were washed once with Hanks' buffer and lysed in 400 μl of 0.01 N HCL in the presence of 0.15 mM EDTA. Norepinephrine levels in the cleared supernatants were

determined by Norepinephrine Research ELISA Kits (Rocky Mountain Diagnostics). Nonmalignant AGCC line tsAM5NE cells were lysed with repeated (three times) freezing–thawing after being transfected with siRNAs. Norepinephrine levels in the cleared supernatants were determined by noradrenaline ELISA kits (LifeSpan BioScernces, Seattle, WA; LS-F10598) according to the manufacturer's instructions. Samples were assayed in duplicate.

Quantitative RT-PCR (RT-qPCR)

mRNA levels of TH and *Egr1* were measured by RT-qPCR. Total RNA from adrenal gland medullar cells or tsAM5NE cells was extracted with TRIzol® (Invitrogen) and reverse-transcribed with the iScript™ cDNA Synthesis Kit (Bio-Rad). Table S1 lists the qPCR primers used. qPCR conditions were as follows: 2 min at 50 °C and 2 min at 95 °C, followed by 40 cycles of 10 s at 94 °C, 20 s at 58 °C, and 20 s at 72 °C. β-Actin mRNA levels were considered internal controls. qPCR signals between 22 and 30 cycles were analyzed. Samples were tested in triplicate, and the data were expressed as signal ratios of target RNA/β-actin mRNA.

Immunoblotting

Adrenal gland medullae were isolated from 8- to 10-week old male mice and cultured in Opti-MEM™ reduced serum medium (Thermo Fisher Scientific, Burlington, ON, Canada; catalog no. 31985070) at 37 °C for 2 h. In some experiments, nicotine (20 μM) (Sigma-Aldrich, Winston, ON, Canada; N3876) was used to stimulate the medullae for 2.5 and 5 min after the 2-h culture period. The tissues were then lysed with radioimmune precipitation assay buffer, which contained PhosSTOP and protease inhibitor mixtures (Roche Applied Science, Meylan Cedex, France). tsAM5NE cells were lysed with radioimmune precipitation assay buffer 72 h after being transfected with *Egr1* siRNA or 4 h after nicotine (40 μM) stimulation in coated plates. 40 μg of lysate protein per sample was resolved on 10% SDS-PAGE. Proteins were transferred from the gel to PVDF membranes (Invitrogen), which were then incubated in blocking buffer containing 5% (w/v) skim milk or 5% BSA for 1 h at room temperature. The membranes were incubated overnight at 4 °C with rabbit anti-TH Ab (2792, Cell Signaling Technology), rabbit anti-EGR1 Ab (ab182624, Abcam), rabbit anti-MKK7 (phospho-Ser^{277}+Thr^{275}) Ab (ab78148, Abcam), rabbit anti-MKK7 Ab (4172, Cell Signaling Technology), rabbit anti-phospho-c-Jun (Ser^{63}) Ab (9261, Cell Signaling Technology), rabbit anti-c-Jun monoclonal Ab (9165, Cell Signaling Technology), rabbit anti-phospho-JNK (Thr^{183}/Tyr^{185}) Ab (9251, Cell Signaling Technology), rabbit anti-JNK Ab (9252, Cell Signaling Technology), mouse anti-phospho-ERK1/2 (Thr^{202}/Tyr^{204}) Ab (9106, Cell Signaling Technology), rabbit anti-ERK1/2 Ab (9102, Cell Signaling Technology), rabbit anti-phospho-p38MAPK (Thy^{180}/Tyr^{182}) Ab (9211, Cell Signaling Technology), rabbit anti-p38MAPK Ab (9212, Cell Signaling Technology), rabbit anti-phospho-ELK1 (Ser^{383}) Ab (ab218133, Abcam), rabbit anti-ELK1 Ab (9182, Cell Signaling Technology), and rabbit anti-β-actin Ab (4967, Cell Signaling Technology). Blots were washed and then incubated with horseradish peroxidase-conjugated secondary Abs for 2 h. All antibodies were used at the manufacturers' recommended dilutions. Signals were visualized using SuperSignal West Pico Chemiluminescent Substrate (Thermo Fisher Scientific).

Adrenal gland medulla organ culture

Adrenal gland medullae were isolated from 8- to 10-week old *Ephb6* KO and WT mice and cultured in DMEM with 15% FCS at 37 °C for 0, 2.5, and 5 min after nicotine (20 μM) stimulation. The medullae were harvested for subsequent EMSA or immunoblotting. For some experiments, they were cultured for 4 h in the presence of RAC1 inhibitor (50 μM, 53502, Sigma-Aldrich), MKK7 inhibitor (50 μM, 335140001, Sigma-Aldrich), the JNK inhibitor SP600125 (20 μM, S5567, Sigma-Aldrich), or vehicle. The medullae were then harvested for the measurement of *Egr1* mRNA levels by RT-qPCR.

DNA microarray

Total RNA was extracted using the RNeasy Mini Kit (74104, Qiagen, Toronto, ON, Canada) from adrenal glands of male, female, and castrated male *Ephb6* KO mice and their WT counterparts. Three biological replicates using different mice for each group were employed. The RNA was quantified using a NanoDrop ND-1000 spectrophotometer (NanoDrop Technologies, Inc.), and its integrity was assessed using a 2100 Bioanalyzer (Agilent Technologies). Double-stranded complementary DNA was synthetized from 250 ng of total RNA, and *in vitro* transcription was performed to produce biotin-labeled cRNA using the Illumina® TotalPrep RNA Amplification Kit according to the manufacturer's instructions (Life Technologies). The labeled cRNA was normalized at 1,500 ng and hybridized on the MouseWG-6_V2 array according to Illumina's Whole-Genome Gene Expression Direct Hybridization Assay Guide. The BeadChips were incubated in an Illumina hybridization oven at 58 °C for 16 h at a standard rocking speed of 5 according to the oven speedometer. BeadChips were washed according to the Illumina protocol mentioned previously and scanned on an Illumina iScan reader.

Mean expression signal levels of all the genes of three replicates in each group were first obtained. Using the mean expression signal level of each gene of the male WT group for comparison, genes with more than 2-fold changes in their expression in the male KO groups were selected. The -fold changes of these selected genes in the female KO group with respect to the female WT group and the -fold changes of these genes in the castrated male KO group with respect to the castrated WT group were calculated and presented.

GTPase activation assay for RAC1

Activated RAC1 G-protein within samples (25 μg/sample) was determined by the G-LISA assay (Cytoskeleton, Inc.), performed according to the manufacturer's instructions. Briefly, adrenal gland medullae were isolated from 8- to 10-week-old *Ephb6* KO and WT mice and cultured in Opti-MEM™ reduced serum medium at 37 °C for 2 h. Nicotine (20 μM) was used to stimulate the adrenal medulla for 2.5 min, which we determined in pilot studies to be the peak activation time. Proteins were extracted from the tissues on ice for 5 min in G-LISA cell lysis buffers containing protease inhibitor cocktails (Cyto-

skeleton, Inc.; BK128). The cleared supernatants were snap-frozen in liquid nitrogen and stored at −80 °C until the assay was performed. Samples were assayed in duplicate. Three independent experiments were conducted, and the results were normalized according to the values of WT samples at time 0. The relative RAC1 activity was calculated as follows: relative RAC1 activity = RAC1 activity of a given sample/RAC1 activity of WT cells at time 0.

Chromaffin cell line culture

AGCC line tsAM5NE cells were cultured in collagen IV–coated 24-well flat-bottom plates (Corning, 354430) in DMEM with 15% FCS and G5 supplement (Thermo Fisher Scientific, 17503012) in an environment of 5% CO_2 at 33 °C. In some experiments, these cells were cultured in wells coated with goat anti-EPHB6 Ab (AF611, R&D Systems, Oakville, ON, Canada), normal goat IgG (sc-2028, Santa Cruz Biotechnology, Mississauga, ON, Canada), recombinant EPHB6-Fc (E9777, Sigma-Aldrich), normal human IgG (0150-01, Southern Biotech), rabbit anti-EFNB1 Ab (sc-1011, Santa Cruz Biotechnology), normal rabbit IgG (sc-2027, Santa Cruz Biotechnology), or goat anti-EFNB2 Ab (AF496, R&D Systems) (2 μg/ml during overnight coating at 4 °C) for 24 h. Nicotine (40 μM) was used to stimulate these cells for 4 h.

siRNA transfection

SMARTpool *Egr1* siRNA (M-040286-01-0005), which contained four pairs of siRNA targeting different regions of *Egr1* mRNA, as well as negative control siRNA (D-001206-13-05) were synthesized by Dharmacon (Lafayette, CO). The siRNA sequences are listed in Table S2. tsAM5NE cells at a density of 2×10^5 cells/well in 24-well plates were transfected with siRNAs (30 nM) with DharmaFECT 1 transfection reagent (Dharmacon, T-2001-02) immediately after passage. The transfected cells were cultured for an additional 24 to 72 h before further manipulation.

EMSA and EMSA immunoblotting

Ephb6 KO and WT male mice were subcutaneously injected with nicotine in PBS (2 mg/kg of body weight) or an equal volume of PBS as a control. The mice were placed in an incubator to prevent hypothermia. After 2 h, their adrenal medullae were isolated, and nuclear proteins were extracted with NE-PER™ nuclear and cytoplasmic extraction reagents (Thermo Fisher Scientific, 78833). EMSAs were performed according to the manufacturer's protocols (Odyssey IR EMSA kit; LI-COR Biosciences, Lincoln, NE). Duplexed oligonucleotides (5′-GGACTTAGGACTGACCTAGAACAATCA-3′) containing the AP-1–binding sequence (positions +383 to +393) in the 5′ UTR of the mouse *Egr1* gene were labeled at the 5′ end with IRDye 800 IR dye (Integrated DNA Technologies, Skokie, IL) and used as probes. The extracted nuclear protein (10 μg) was incubated with 5 nM IRdye800-labeled probes for 30 min. For background control, a 200-fold molar excess of unlabeled probes was added to a sample containing WT nuclear extracts to determine the background association of the probes with the nuclear proteins. DNA–protein mixtures were separated by 5% nondenaturing PAGE in 0.5× Tris borate–EDTA buffer. Gels were imaged using the LI-COR Odyssey imaging system. The specific AP-1–binding activity was calculated as follows: AP-1–binding activity = AP-1 signal of testing samples − signal of the background control. For each experiment, the AP-1–binding activity of WT cells without nicotine stimulation (*i.e.* treated with PBS) was used to normalize the values of all other samples to calculate their respective normalized relative AP-1–binding activity using the following formula: normalized relative AP-1–binding activity = the specific AP-1–binding activity of a given sample/the specific AP-1–binding activity of WT samples treated with PBS.

To identify c-JUN and c-FOS proteins in the shifted bands, proteins in nondenaturing polyacrylamide gels of the EMSA were transferred to PVDF membranes. The membranes were blocked with PBS containing 5% (w/v) skim milk for 1 h at room temperature. They were then reacted overnight at 4 °C with rabbit anti-c-Jun mAb (9165, Cell Signaling Technology) or rabbit anti-c-Fos Ab (ab190289, Abcam). The membranes were washed and then incubated with horseradish peroxidase–conjugated secondary Ab for 2 h. All Abs were used at the manufacturers' recommended dilutions. Signals were visualized using SuperSignal West Pico Chemiluminescent Substrate (Thermo Fisher Scientific).

Primary AGCC culture

Primary mouse AGCCs were isolated as described previously (23). Briefly, adrenal gland medullae were obtained from 8- to 10-week-old mice. Papain (P4762, Sigma-Aldrich) was activated with 5 mM L-cysteine. The medullae were digested by the activated papain in Hanks' buffer at 37 °C for 25 min. They were washed twice with Hanks' buffer and then triturated by pipetting in 300 μl of Hanks' buffer until they became feather-like. Cells were pelleted at 3,700 × *g* for 3 min and resuspended in DMEM containing 15% (v/v) FCS for culture. BSA-conjugated testosterone (1.1 μg/ml, Aviva Systems Biology, San Diego, CA) or BSA was added to the culture 15 min prior to addition of nicotine (20 μM), and the cells were cultured for 16 h at 37 °C before being harvested for norepinephrine content measurement.

Ethics statement

All animal studies were approved by the Animal Protection Committee (Comité institutionnel d'intégration de la protection des animaux) of Centre de recherche, Centre hospitalier de l'Université de Montréal.

Author contributions—W. S., Y. W., N. V., H. L., and J. W. conceptualization; W. S. and Y. W. data curation; W. S., Y. W., and J. W. formal analysis; W. S., Y. W., and H. L. investigation; W. S., Y. W., J. P., and S. Q. methodology; W. S. and J. W. writing-original draft; N. K. and T. M. resources; H. L. and J. W. supervision; H. L. and J. W. project administration; J. W. funding acquisition.

References

1. Eph Nomenclature Committee (1997) Unified nomenclature for Eph family receptors and their ligands, the ephrins. *Cell* **90,** 403–404 CrossRef Medline
2. Pasquale, E. B. (2008) Eph-ephrin bidirectional signaling in physiology and disease. *Cell* **133,** 38–52 CrossRef Medline

3. Luo, H., Wan, X., Wu, Y., and Wu, J. (2001) Cross-linking of EphB6 resulting in signal transduction and apoptosis in Jurkat cells. *J. Immunol.* **167,** 1362–1370 CrossRef Medline
4. Luo, H., Yu, G., Wu, Y., and Wu, J. (2002) EphB6 crosslinking results in costimulation of T cells. *J. Clin. Invest.* **110,** 1141–1150 CrossRef Medline
5. Yu, G., Luo, H., Wu, Y., and Wu, J. (2003) Ephrin B2 induces T cell costimulation. *J. Immunol.* **171,** 106–114 CrossRef Medline
6. Yu, G., Luo, H., Wu, Y., and Wu, J. (2003) Mouse ephrinB3 augments T-cell signaling and responses to T-cell receptor ligation. *J. Biol. Chem.* **278,** 47209–47216 CrossRef Medline
7. Luo, H., Yu, G., Tremblay, J., and Wu, J. (2004) EphB6-null mutation results in compromised T cell function. *J. Clin. Invest.* **114,** 1762–1773 CrossRef Medline
8. Yu, G., Luo, H., Wu, Y., and Wu, J. (2004) EphrinB1 is essential in T-cell–T-cell co-operation during T-cell activation. *J. Biol. Chem.* **279,** 55531–55539 CrossRef Medline
9. Wu, J., and Luo, H. (2005) Recent advances on T-cell regulation by receptor tyrosine kinases. *Curr. Opin. Hematol.* **12,** 292–297 CrossRef Medline
10. Yu, G., Mao, J., Wu, Y., Luo, H., and Wu, J. (2006) Ephrin-B1 is critical in T-cell development. *J. Biol. Chem.* **281,** 10222–10229 CrossRef Medline
11. Luo, H., Wu, Z., Qi, S., Jin, W., Han, B., and Wu, J. (2011) EFNB1 and EFNB2 physically bind to IL-7 receptor α and retard its internalization from the cell surface. *J. Biol. Chem.* **286,** 44976–44987 CrossRef Medline
12. Luo, H., Charpentier, T., Wang, X., Qi, S., Han, B., Wu, T., Terra, R., Lamarre, A., and Wu, J. (2011) Efnb1 and Efnb2 proteins regulate thymocyte development, peripheral T cell differentiation, and antiviral immune responses and are essential for interleukin-6 (IL-6) signaling. *J. Biol. Chem.* **286,** 41135–41152 CrossRef Medline
13. Jin, W., Luo, H., and Wu, J. (2014) Effect of reduced EPHB4 expression in thymic epithelial cells on thymocyte development and peripheral T cell function. *Mol. Immunol.* **58,** 1–9 CrossRef Medline
14. Hu, Y., Wang, X., Wu, Y., Jin, W., Cheng, B., Fang, X., Martel-Pelletier, J., Kapoor, M., Peng, J., Qi, S., Shi, G., Wu, J., and Luo, H. (2015) Role of EFNB1 and EFNB2 in mouse collagen-induced arthritis and human rheumatoid arthritis. *Arthritis Rheumatol.* **67,** 1778–1788 CrossRef Medline
15. Luo, H., Broux, B., Wang, X., Hu, Y., Ghannam, S., Jin, W., Larochelle, C., Prat, A., and Wu, J. (2016) EphrinB1 and EphrinB2 regulate T cell chemotaxis and migration in experimental autoimmune encephalomyelitis and multiple sclerosis. *Neurobiol. Dis.* **91,** 292–306 CrossRef Medline
16. Luo, H., Wu, Z., Tremblay, J., Thorin, E., Peng, J., Lavoie, J. L., Hu, B., Stoyanova, E., Cloutier, G., Qi, S., Wu, T., Cameron, M., and Wu, J. (2012) Receptor tyrosine kinase Ephb6 regulates vascular smooth muscle contractility and modulates blood pressure in concert with sex hormones. *J. Biol. Chem.* **287,** 6819–6829 CrossRef Medline
17. Wu, Z., Luo, H., Thorin, E., Tremblay, J., Peng, J., Lavoie, J. L., Wang, Y., Qi, S., Wu, T., and Wu, J. (2012) Possible role of Efnb1 protein, a ligand of Eph receptor tyrosine kinases, in modulating blood pressure. *J. Biol. Chem.* **287,** 15557–15569 CrossRef Medline
18. Wang, Y., Thorin, E., Luo, H., Tremblay, J., Lavoie, J. L., Wu, Z., Peng, J., Qi, S., and Wu, J. (2015) EPHB4 protein expression in vascular smooth muscle cells regulates their contractility, and EPHB4 deletion leads to hypotension in mice. *J. Biol. Chem.* **290,** 14235–14244 CrossRef Medline
19. Wang, Y., Hamet, P., Thorin, E., Tremblay, J., Raelson, J., Wu, Z., Luo, H., Jin, W., Lavoie, J. L., Peng, J., Marois-Blanchet, F. C., Tahir, M. R., Chalmers, J., Woodward, M., Harrap, S., *et al.* (2016) Reduced blood pressure after smooth muscle EFNB2 deletion and the potential association of EFNB2 mutation with human hypertension risk. *Eur. J. Hum. Genet.* **24,** 1817–1825 CrossRef Medline
20. Wang, Y., Wu, Z., Thorin, E., Tremblay, J., Lavoie, J. L., Luo, H., Peng, J., Qi, S., Wu, T., Chen, F., Shen, J., Hu, S., and Wu, J. (2016) Estrogen and testosterone in concert with EFNB3 regulate vascular smooth muscle cell contractility and blood pressure. *Am. J. Physiol. Heart Circ. Physiol.* **310,** H861-H872 CrossRef Medline
21. Wang, Y., Wu, Z., Luo, H., Peng, J., Raelson, J., Ehret, G. B., Munroe, P. B., Stoyanova, E., Qin, Z., Cloutier, G., Bradley, W. E., Wu, T., Shen, J. Z., Hu, S., and Wu, J. (2016) The role of GRIP1 and ephrin B3 in blood pressure control and vascular smooth muscle cell contractility. *Sci. Rep.* **6,** 38976 CrossRef Medline
22. Tremblay, J., Wang, Y., Raelson, J., Marois-Blanchet, F. C., Wu, Z., Luo, H., Bradley, E., Chalmers, J., Woodward, M., Harrap, S., Hamet, P., and Wu, J. (2017) Evidence from single nucleotide polymorphism analyses of ADVANCE study demonstrates EFNB3 as a hypertension risk gene. *Sci. Rep.* **7,** 44114 CrossRef Medline
23. Wang, Y., Shi, W., Blanchette, A., Peng, J., Qi, S., Luo, H., Ledoux, J., and Wu, J. (2018) EPHB6 and testosterone in concert regulate epinephrine release by adrenal gland chromaffin cells. *Sci. Rep.* **8,** 842 CrossRef Medline
24. Wu, T., Zhang, B. Q., Raelson, J., Yao, Y. M., Wu, H. D., Xu, Z. X., Marois-Blanchet, F. C., Tahir, M. R., Wang, Y., Bradley, W. E., Luo, H., Wu, J., Sheng, J. Z., and Hu, S. J. (2018) Analysis of the association of EPHB6, EFNB1 and EFNB3 variants with hypertension risks in males with hypogonadism. *Sci. Rep.* **8,** 14497 CrossRef Medline
25. Zhang, Z., Tremblay, J., Raelson, J., Sofer, T., Du, L., Fang, Q., Argos, M., Marois-Blanchet, F. C., Wang, Y., Yan, L., Chalmers, J., Woodward, M., Harrap, S., Hamet, P., Luo, H., and Wu, J. (2019) EPHA4 regulates vascular smooth muscle cell contractility and is a hypertension risk gene. *J. Hypertens.* **37,** 775–789 CrossRef Medline
26. James, G. D., and Brown, D. E. (1997) The biological stress response and lifestyle: catecholamines and blood pressure. *Annu. Rev. Anthropol.* **26,** 313–335 CrossRef
27. de Champlain, J., Farley, L., Cousineau, D., and van Ameringen, M. R. (1976) Circulating catecholamine levels in human and experimental hypertension. *Circ. Res.* **38,** 109–114 CrossRef Medline
28. Kohno, S., Murata, T., Koide, N., Hikita, K., and Kaneda, N. (2011) Establishment and characterization of a noradrenergic adrenal chromaffin cell line, tsAM5NE, immortalized with the temperature-sensitive SV40 T-antigen. *Cell Biol. Int.* **35,** 325–334 CrossRef Medline
29. Hess, J., Angel, P., and Schorpp-Kistner, M. (2004) AP-1 subunits: quarrel and harmony among siblings. *J. Cell Sci.* **117,** 5965–5973 CrossRef Medline
30. Gasman, S., Chasserot-Golaz, S., Bader, M. F., and Vitale, N. (2003) Regulation of exocytosis in adrenal chromaffin cells: focus on ARF and Rho GTPases. *Cell Signal.* **15,** 893–899 CrossRef Medline
31. Wong, D. L., and Tank, A. W. (2007) Stress-induced catecholaminergic function: transcriptional and post-transcriptional control. *Stress* **10,** 121–130 CrossRef Medline
32. Dunkley, P. R., Bobrovskaya, L., Graham, M. E., von Nagy-Felsobuki, E. I., and Dickson, P. W. (2004) Tyrosine hydroxylase phosphorylation: regulation and consequences. *J. Neurochem.* **91,** 1025–1043 CrossRef Medline
33. Daubner, S. C., Le, T., and Wang, S. (2011) Tyrosine hydroxylase and regulation of dopamine synthesis. *Arch. Biochem. Biophys.* **508,** 1–12 CrossRef Medline
34. Papanikolaou, N. A., and Sabban, E. L. (2000) Ability of Egr1 to activate tyrosine hydroxylase transcription in PC12 cells: cross-talk with AP-1 factors. *J. Biol. Chem.* **275,** 26683–26689 Medline
35. Cruzalegui, F. H., Cano, E., and Treisman, R. (1999) ERK activation induces phosphorylation of Elk-1 at multiple S/T-P motifs to high stoichiometry. *Oncogene* **18,** 7948–7957 CrossRef Medline
36. Hoffmann, E., Ashouri, J., Wolter, S., Doerrie, A., Dittrich-Breiholz, O., Schneider, H., Wagner, E. F., Troppmair, J., Mackman, N., and Kracht, M. (2008) Transcriptional regulation of EGR-1 by the interleukin-1-JNK-MKK7-c-Jun pathway. *J. Biol. Chem.* **283,** 12120–12128 CrossRef Medline
37. Lee, W., Haslinger, A., Karin, M., and Tjian, R. (1987) Activation of transcription by two factors that bind promoter and enhancer sequences of the human metallothionein gene and SV40. *Nature* **325,** 368–372 CrossRef Medline
38. Shaulian, E., and Karin, M. (2002) AP-1 as a regulator of cell life and death. *Nat. Cell Biol.* **4,** E131–136 CrossRef Medline
39. Kouzarides, T., and Ziff, E. (1988) The role of the leucine zipper in the Fos-Jun interaction. *Nature* **336,** 646–651 CrossRef Medline
40. Nakabeppu, Y., Ryder, K., and Nathans, D. (1988) DNA binding activities of three murine Jun proteins: stimulation by Fos. *Cell* **55,** 907–915 CrossRef Medline
41. Davis, R. J. (2000) Signal transduction by the JNK group of MAP kinases. *Cell* **103,** 239–252 CrossRef Medline

42. Schreck, I., Al-Rawi, M., Mingot, J. M., Scholl, C., Diefenbacher, M. E., O'Donnell, P., Bohmann, D., and Weiss, C. (2011) c-Jun localizes to the nucleus independent of its phosphorylation by and interaction with JNK and vice versa promotes nuclear accumulation of JNK. *Biochem. Biophys. Res. Commun.* **407,** 735–740 CrossRef Medline
43. Ip, Y. T., and Davis, R. J. (1998) Signal transduction by the c-Jun N-terminal kinase (JNK): from inflammation to development. *Curr. Opin. Cell Biol.* **10,** 205–219 CrossRef Medline
44. Foltz, I. N., Gerl, R. E., Wieler, J. S., Luckach, M., Salmon, R. A., and Schrader, J. W. (1998) Human mitogen-activated protein kinase 7 (MKK7) is a highly conserved c-Jun N-terminal kinase/stress-activated protein kinase (JNK/SAPK) activated by environmental stresses and physiological stimuli. *J. Biol. Chem.* **273,** 9344–9351 CrossRef Medline
45. Wang, X., Destrument, A., and Tournier, C. (2007) Physiological roles of MKK4 and MKK7: insights from animal models. *Biochim. Biophys. Acta* **1773,** 1349–1357 CrossRef Medline
46. Holtmann, H., Winzen, R., Holland, P., Eickemeier, S., Hoffmann, E., Wallach, D., Malinin, N. L., Cooper, J. A., Resch, K., and Kracht, M. (1999) Induction of interleukin-8 synthesis integrates effects on transcription and mRNA degradation from at least three different cytokine- or stress-activated signal transduction pathways. *Mol. Cell. Biol.* **19,** 6742–6753 CrossRef Medline
47. Holland, P. M., Suzanne, M., Campbell, J. S., Noselli, S., and Cooper, J. A. (1997) MKK7 is a stress-activated mitogen-activated protein kinase kinase functionally related to hemipterous. *J. Biol. Chem.* **272,** 24994–24998 CrossRef Medline
48. Nakada, M., Drake, K. L., Nakada, S., Niska, J. A., and Berens, M. E. (2006) Ephrin-B3 ligand promotes glioma invasion through activation of Rac1. *Cancer Res.* **66,** 8492–8500 CrossRef Medline
49. O'Neill, A. K., Kindberg, A. A., Niethamer, T. K., Larson, A. R., Ho, H. H., Greenberg, M. E., and Bush, J. O. (2016) Unidirectional Eph/ephrin signaling creates a cortical actomyosin differential to drive cell segregation. *J. Cell Biol.* **215,** 217–229 CrossRef Medline
50. Nakayama, A., Nakayama, M., Turner, C. J., Höing, S., Lepore, J. J., and Adams, R. H. (2013) Ephrin-B2 controls PDGFRβ internalization and signaling. *Genes Dev.* **27,** 2576–2589 CrossRef Medline
51. Gregg, J., and Fraizer, G. (2011) Transcriptional regulation of EGR1 by EGF and the ERK signaling pathway in prostate cancer cells. *Genes Cancer* **2,** 900–909 CrossRef Medline
52. Hipskind, R. A., Rao, V. N., Mueller, C. G., Reddy, E. S., and Nordheim, A. (1991) Ets-related protein Elk-1 is homologous to the c-fos regulatory factor p62TCF. *Nature* **354,** 531–534 CrossRef Medline
53. Yang, S. H., Jaffray, E., Hay, R. T., and Sharrocks, A. D. (2003) Dynamic interplay of the SUMO and ERK pathways in regulating Elk-1 transcriptional activity. *Mol. Cell* **12,** 63–74 CrossRef Medline
54. Rao, V. N., Huebner, K., Isobe, M., ar-Rushdi, A., Croce, C. M., and Reddy, E. S. (1989) Elk, tissue-specific ets-related genes on chromosomes X and 14 near translocation breakpoints. *Science* **244,** 66–70 CrossRef Medline